8. SITE 297

The Shipboard Scientific Party[1]

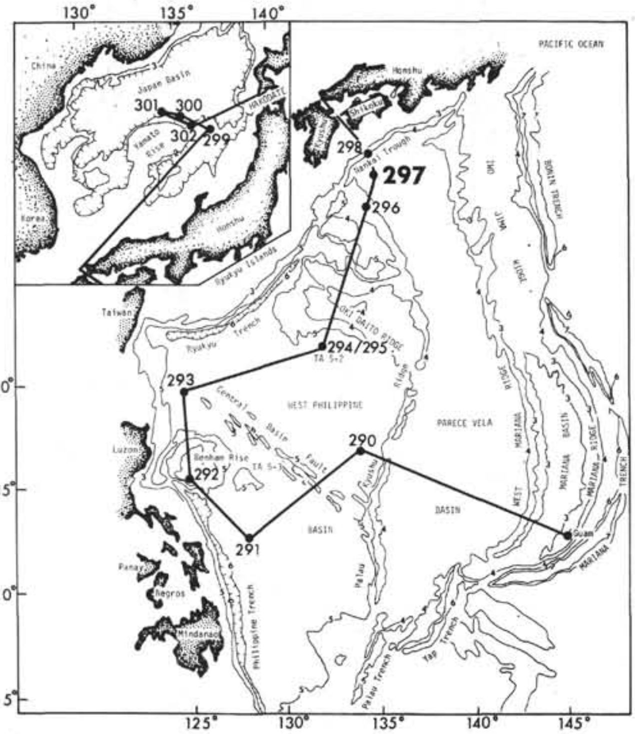

Figure 1. *Location of Site 297 and track of* Glomar Challenger. *"Topography of North Pacific," T. E. Chase, H. W. Menard, and J. Mammerickx, Institute Marine Resources, Geol. Data Center, Scripps Institution of Oceanography, 1971. Contour depths in kilometers. Scale 1:6,500,000.*

SITE DATA

Position: 30°52.36′N; 134°09.89′E

Water Depth (from sea level): 4458 corrected meters (echo sounding)

Bottom Felt At: 4480.5 meters (drillpipe)

Penetration:
Hole 297: 679.5 meters
Hole 297A: 200.5 meters

Number of Holes: 2

Number of Cores:
Hole 297: 27
Hole 297A: 0

Total Length of Cored Section:
Hole 297: 242.5 meters
Hole 297A: 0 meters

Total Core Recovered: 124.2 meters

Percentage of Core Recovery: 51.2%

Oldest Sediment Cored:
Depth below sea floor: 679.5 meters
Nature: Vitric ash and ash-rich claystone
Age: Early mid Miocene or late early Miocene
Inferred depth to basement: 780 meters

Principal Results: Site 297 is located in the northwestern corner of the Shikoku Basin directly south of the Nankai Trough and Shikoku Island. The stratigraphic section consists of 54 meters of Pleistocene diatom/ash-rich clay, 36 meters of Pleistocene clay-rich nannofossil ooze, 240 meters of Pleistocene-late Pliocene claystone, 247 meters of late-early Pliocene claystone and turbidite sands and silts with displaced shallow-water foraminifera, and 122 meters of early Pliocene(?) to middle Miocene vitric ash and claystone. Cessation of turbidite deposition of continental material including plant debris in early Pliocene, probably marks formation of the Nankai Trough, and an increase in rate of subduction in this trench. Although basement was not reached due to technical difficulties, seismic reflection and refraction data indicate that basalt lies approximately 780 meters below the bottom of the hole and is of early Miocene age.

BACKGROUND AND OBJECTIVES

Background

Although a site was not originally planned in the Shikoku Basin, the restrictions imposed on the basis of safety and pollution criteria for the proposed hole high on the continental slope of Japan and the accomplishment at Site 296 of many of the biostratigraphic objectives of the slope hole made a basin hole preferable. Site 297 lay in the north central part of the basin and on the outer arch of the Nankai Trough (Figures 1 and 2). The Shikoku Basin lies east of the Palau-Kyushu Ridge and is joined at its south end with the Parece Vela Basin, in which probable late Oligocene or early Miocene basement was drilled on DSDP Leg 6 (Fischer et al., 1971). Prior to Leg 31, however, it was not known whether or not the two basins represented the same pulse of crustal

---

[1] James C. Ingle, Jr., Stanford University, Stanford, California; Daniel E. Karig, Cornell University, Ithaca, New York; Arnold H. Bouma, Texas A&M University, College Station, Texas; C. Howard Ellis, Marathon Oil Company, Littleton, Colorado; Neville S. Haile, University of Malaya, Kuala Lumpur, Malaysia; Itaru Koizumi, Osaka University, Osaka, Japan; Ian MacGregor, University of California at Davis, Davis, California; J. Casey Moore, University of California at Santa Cruz; Santa Cruz, California; Hiroshi Ujiié, National Science Museum of Tokyo, Tokyo, Japan; Teruhiko Watanabe, University of Tokyo, Tokyo, Japan; Stan M. White, California State University at Fresno, Fresno, California; Masashi Yasui, Japan Meteorological College, Tokyo, Japan; Hsin Yi Ling, University of Washington, Seattle, Washington.

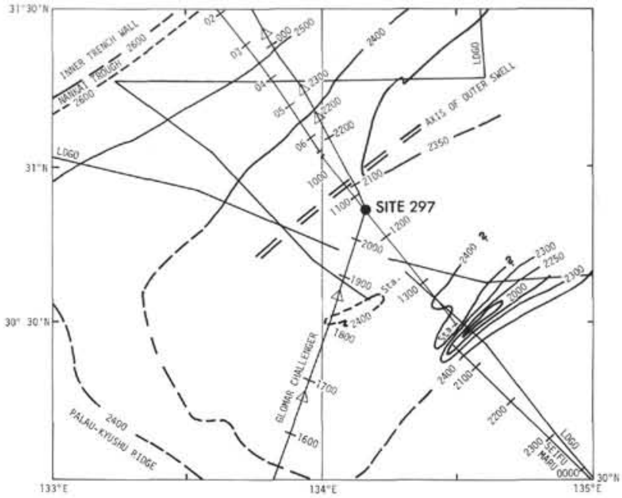

Figure 2. *Preliminary bathymetry near Site 297, based on recent well-navigated cruise tracks and data from Chase et al. (1969). Depth is in uncorrected fathoms (400/m = 1 sec 2-way travel time).*

extension. Heat flow-depth age relations, which seem to be qualitatively valid in marginal basins (Karig, 1971; Sclater, 1972), suggest that the Shikoku Basin is of mid-Tertiary age. The cessation of volcanic activity at Site 296 on the Palau-Kyushu Ridge, if attributable to the shifting of the volcanic source as the Shikoku Basin opened, is indicative of a late Oligocene basin initiation.

The age and history of the Shikoku Basin is also relevant to the understanding of the development of the southwest Japan continental margin, which has intermittently been subjected to subduction since at least the late Paleozoic. The last major pulse of subduction apparently formed the Shimanto zone of highly deformed sediments in the Late Cretaceous and persisted into the early Tertiary when tectonic and volcanic effects died out. The present existence of a shallow trench (Nankai Trough) and associated seismicity restricted to shallow focus earthquakes has led to the conclusion that a new pulse of subduction began 1 to 2 million years ago (Hilde et al., 1969; Fitch and Scholz, 1971; Kanimori, 1972).

Before the trench developed, the turbidites, which now collect in the trench axis, should have been able to spread out across the Shikoku Basin. Thus a switch in sedimentation regime, from turbidites to pelagics should correspond to the initiation of the trench as a morphologic depression. Seismic reflection profiles (Figure 3) outline a 700-800 meter thick sediment column in the northern part of the Shikoku Basin, and shows this sedimentological transition at a depth near 350 meters.

Site 297 was positioned on the outer arch of the trench and was located along a seismic reflection profile obtained by the R/V *Seifu Maru* of the Maizuru Marine Observatory (Figure 4).

Objectives

Determination of the age and nature of the basement and of the basal sediments in the basin was necessary for the tectonic reconstruction of the eastern Philippine Sea and to test the validity of the extensional origin of marginal basins. The age and sedimentary character of the stratigraphic column was expected to reveal the date of initiation of the Nankai Trough and hopefully to elucidate uplift, subsidence, and volcanic histories of southwest Japan and the Palau-Kyushu Ridge.

OPERATIONS

Presite Survey

Accumulated extra time from previous sites, together with a decision not to drill a proposed site on the Tosa Terrace, allowed unscheduled Site 297 to be drilled at the westernmost corner of the Shikoku Basin. Location of this site was based upon May 1970 seismic records of the *Seifu Maru* (Figure 4) along a track closely paralleling the route to proposed Site 298 in the Nankai Trough. It was decided information at Site 297 would almost certainly bear directly on the origin of the Palau-Kyushu Ridge, the Nankai Trough, and Shikoku Basin proper.

The older Japanese seismic records illustrated that the western Shikoku Basin is typically covered by about 0.8 sec of relatively transparent sediment. This same unit of undulating sediment was clearly seen on *Glomar Challenger* records after passing across the eastern flank of the Palau-Kyushu Ridge onto the plain of Shikoku Basin. The proposed site area was approached along 018° at 9 knots (Figures 2 and 3). After slowing to 7 knots, a 16-kHz beacon was released at 0500, 15 July at a depth of 4458 meters on the outer swell of the Nankai Trough.

Drilling Operations

A reasonably good sonobuoy record made at Site 297 prior to drilling displayed four acoustic units: (a) a 0.4-sec transparent layer, (b) a unit of reverberating character between 0.5 and 0.62 sec, (c) an additional transparent layer beginning at 0.62 sec, with (d) a rumpled acoustic basement reflector at 0.83 sec. The drilling program was designed to interval core within each of these units, with closely spaced coring at each acoustic boundary. Hole 297 was spudded at 1415, 15 July.

Cores 1 through 14 (0-324.0 m) penetrated sequences which correlated well with the upper transparent layer seen in seismic records. Heat-flow measurements were made within this interval at 77 meters and 153 meters.

At 333 meters drilling rate increased (Figure 5) as a series of interbedded turbidite sands, silts, and clays was encountered. Core recovery was poor due to loss of sand interbeds. Loss of sands was aided by the necessity of continual circulation, as well as use of mud to maintain the hole and to aid penetration of alternating hard and soft horizons sampled in Cores 15-22 (333.5-561.5 m). It also became apparent that the bumper subs were becoming filled with sand while passing through this sequence.

Drilling rate increased slightly at about 560 meters as an ash-rich clay was encountered, which was sampled in Cores 23-27 (590-679.5 m). This clay correlates with the lower transparent acoustic layer. The bumper subs became inoperative at 679.5 meters (Core 27) due to filling with sand, causing extremely high bit loads in conjunction with large swells. Consequently, Site 297 was abandoned. Table 1 contains a summary of the coring.

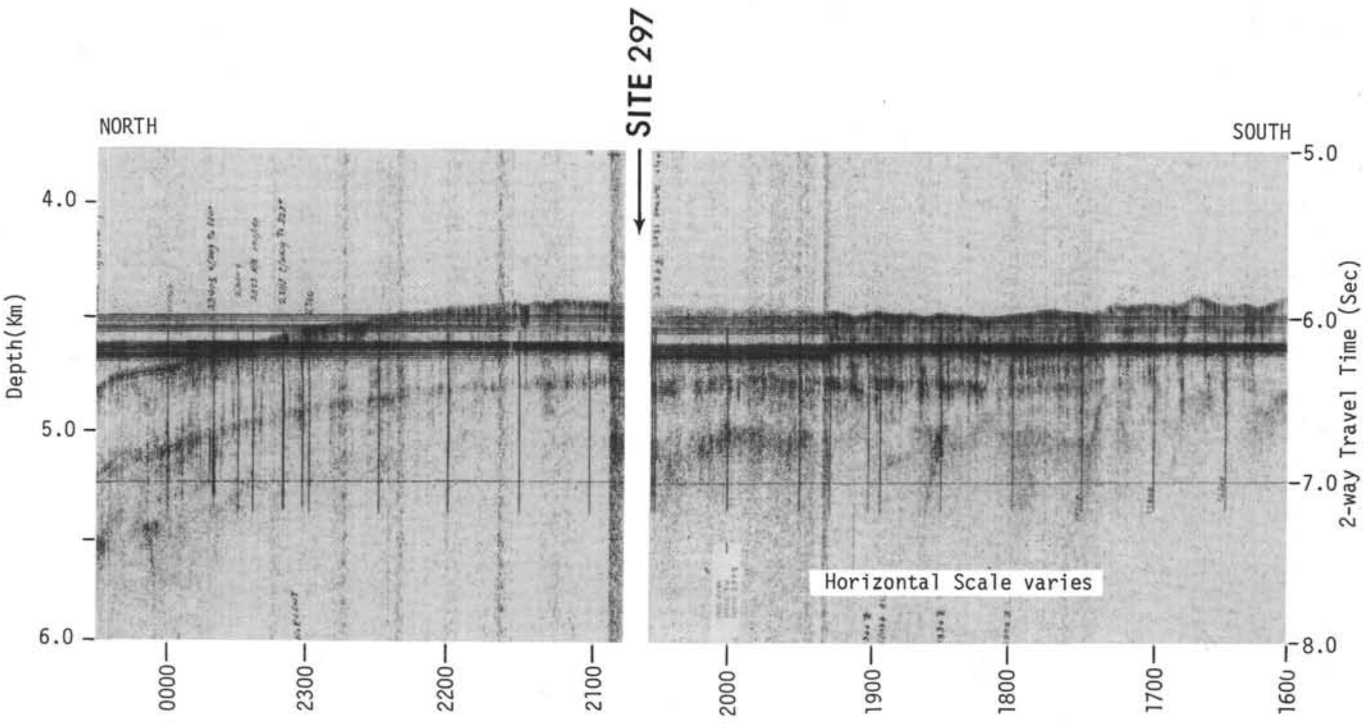

Figure 3. Glomar Challenger *seismic reflection profile approaching and departing Site 297. Profile location is shown on Figure 2.*

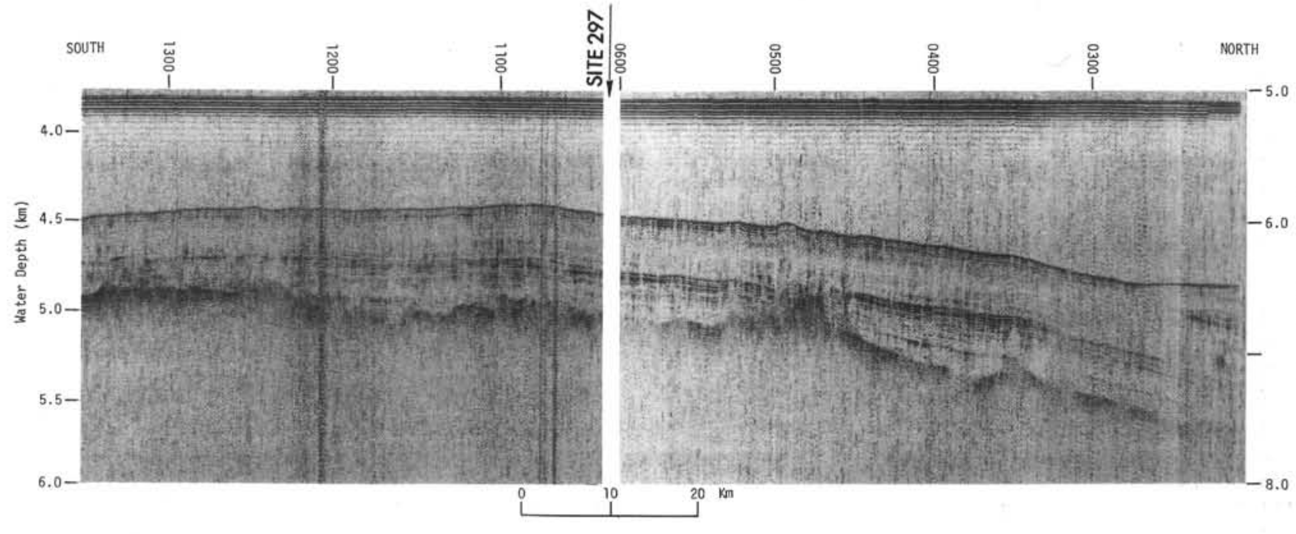

Figure 4. Seifu Maru *(Maizuru Marine Obs.) reflection profile across the outer swell of the Nankai Trough and through Site 297.*

Since one of the major objectives at Site 297 was to obtain a basement age, it was decided that a second hole (297A) would be drilled in order to carry on the interrupted program of Hole 297. Hole 297A was spudded at the same location as Hole 297 at 1000, 18 July. It was planned to wash down to about 650 meters, and then commence interval coring to basement. After washing to 200.5 meters (Table 1), the Bowen power sub failed due to problems in the hydraulic fluid control system. Repairs were unsuccessful. Uncertainty as to the exact nature of the problem, together with time constraints imposed by our schedule for entering the Sea of Japan, caused Hole 297A to be abandoned with no cores taken. Site 297 was departed at 0530, 19 July, and the ship headed for Site 298 in the adjacent Nankai Trough, under threat of typhoon Ellen.

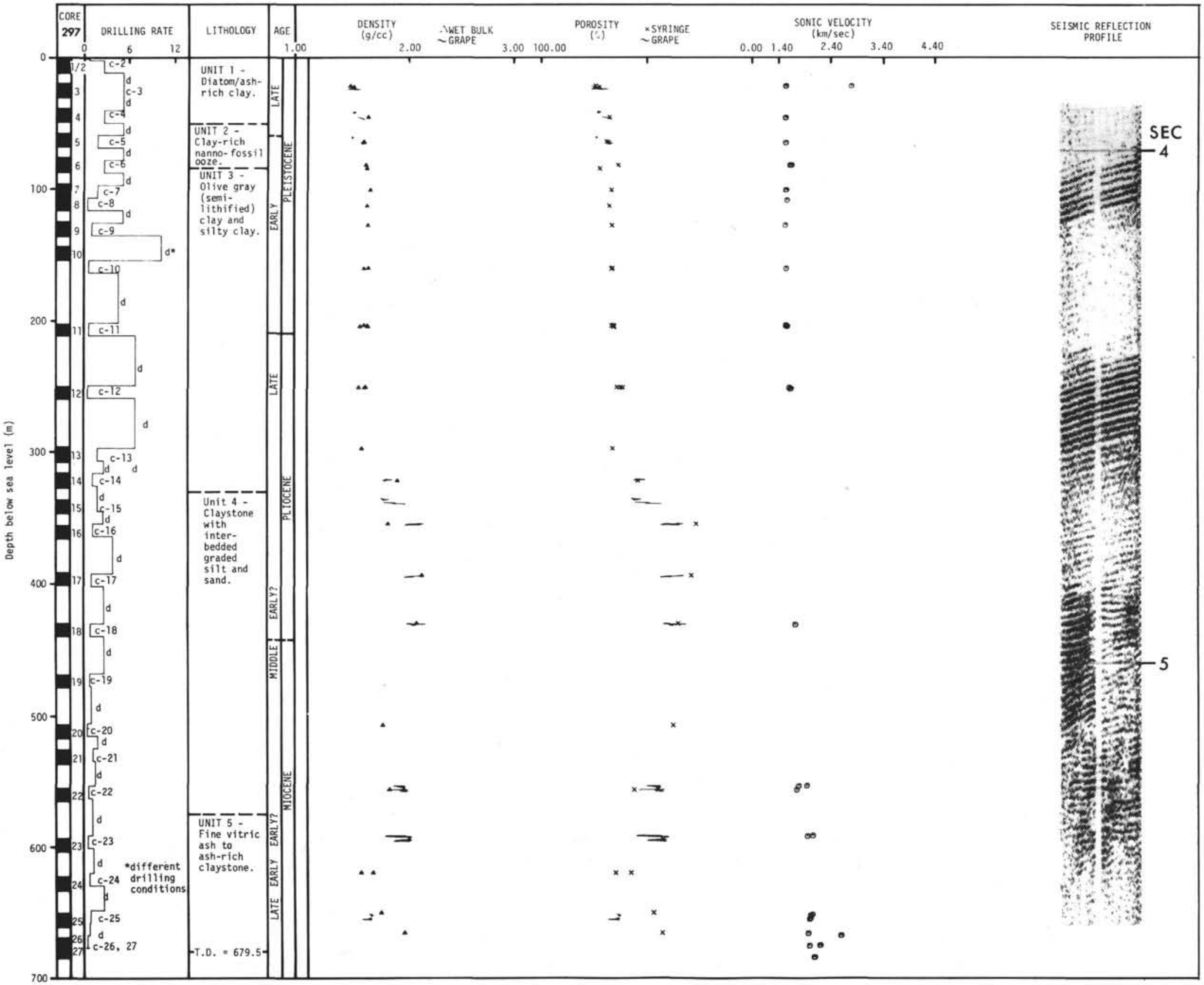

Figure 5. *Hole summary diagram, Site 297.*

TABLE 1
Coring Summary, Site 297

Core	Cored Interval Below Bottom (m)	Cored (m)	Recovered		Remarks[a]
			(m)	(%)	
Hole 297					
1	0.0-1.0	1.0	0.0	0.0	Punch Core
2	1.0-10.5	9.5	0.3		
Wash	10.5-20.0				
3	20.0-29.5	9.5	3.7	39.0	
Wash	29.5-39.0				
4	39.0-48.5	9.5	9.5	100	
Wash	48.5-58.0				
5	58.0-67.5	9.5	9.5	100	
Wash	67.5-77.0				Heat flow taken at 77 meters
6	77.0-86.5	9.5	9.2	97.0	
Wash	86.5-96.0				
7	96.0-105.5	9.5	4.8	51.0	Decrease in drilling rate at 100 meters
8	105.5-115.0	9.5	8.7	92.0	
Wash	115.0-124.5				
9	124.5-134.0	9.5	4.0	43.0	
Wash	134.0-153.0				Heat flow taken at 153 meters
10	153.0-162.5	9.5	8.0	84.0	
Wash	162.5-200.5				
11	200.5-210.0	9.5	5.1	54.0	
Wash	210.0-248.0				
12	248.0-257.5	9.5	3.5	38.0	
Wash	257.5-295.5				
13	295.5-305.0	9.5	1.2	14.0	
Wash	305.0-314.5				
14	314.5-324.0	9.5	9.3	97.0	
Wash	324.0-333.5				Drilling rate increase at 333 meters
15	333.5-343.0	9.5	5.3	56.0	
Wash	343.0-352.5				
16	352.5-362.5	9.5	3.0	32.0	
Wash	362.5-390.5				50 bbls mud
17	390.5-400.0	9.5	3.7	39.0	
Wash	400.0-428.5				
18	428.5-438.0	9.5	3.0	32.0	
Wash	438.0-466.5				
19	466.5-476.0	9.5	0.6	6.0	
Wash	476.0-504.5				50 bbls mud
20	504.4-514.0	9.5	4.2	45.0	
Wash	514.0-523.5				
21	523.5-533.0	9.5	3.2	35.0	
Wash	533.0-552.0				
22	552.0-561.5	9.5	4.8	51.0	Slight increase in drilling rate at 560 meters
Wash	561.5-590.0				
23	590.0-599.5	9.5	5.0	53.0	
Wash	599.5-618.5				
24	618.5-628.0	9.5	3.5	38.0	
Wash	628.0-647.0				
25	647.0-656.5	9.5	8.1	85.0	
Wash	656.5-666.0				
26	666.0-675.5	9.5	2.1	22.0	
27	675.5-679.5	4.0	0.9	23.0	
Total	679.5	242.5	124.2	52.0	
Hole 297A					
Wash	0.0-200.5				
Total	200.5				

[a] See Figure 5 for graph of drilling rate and lithology.

LITHOLOGY

Hole 297 penetrated 697.5 meters below the sea floor. Twenty-seven cores containing 124.2 meters of sediment were recovered. Five units were defined (Table 2 and Figures 5, 6).

Unit 1

This unit, a diatom/ash clay, is characterized by a diatom content ranging from 5% to 44%, with calcareous nannofossils making up less than 1%. This is in contrast to the 15%-72% nannofossils in the underlying Unit 2. Silt-sized glass and volcanogenic feldspar make up 15%-93% of the sediment. Volcanic ash occurs as small pods, and as beds as much as 0.5 meters thick (Core 3, Section 3). The dominant color is olive-gray.

Unit 2

This unit, a clay-rich nannofossil ooze, is characterized by 15%-72% nannofossils, generally becoming more clayey downwards with a decrease in nannofossils, passing into a nannofossil-rich clay. Diatoms are 1% or less. All samples contain some volcanic ash (about 10%-20%) and a few thin lenses of vitric ash are present. The dominant color is medium gray.

Unit 3

Unit 3 is noticeably more consolidated than either Unit 1 or 2 and in general contains little or no ash, although thin ash beds are found in Core 12. It is dominantly an olive-gray semilithified clay, and silty clay, with few fossils.

Unit 4

This unit is characterized by the presence, within the dominant olive-gray to olive-black claystone, of thin (less than 0.3 m) graded beds of silt, and fine sand, presumably turbidites. The sand includes frosted grains of quartz and silt. Fine plant debris is common, pointing to a continental source. Ash and fossils are generally absent, or only present in trace amounts. Some pyrite and glauconite are present.

The most convincing evidence of turbidites is in Core 22, (Sections 2, 3), where graded sands and silts are present in the following sequence:

d = upper interval of parallel lamination
c = interval of convolute lamination and/or cross-bedding
b = lower interval of parallel lamination

distinct contacts
e
d
c
b

indistinct contacts
e
d
c
b

Unit 5

Unit 5 is fine vitric ash to ash-rich claystone and is characterized by abundant to dominant silt-sized, fresh, colorless volcanic glass. Graded beds at the top of the unit are interpreted as distal turbidites and contain pyrite and plant debris at some levels. The vitric ash is laminated, and faint color banding enables minor, but intense, slump structures to be distinguished in several zones. One laminated ash overlies an irregular surface of a graded ash bed; the irregularities of this surface apparently were caused by minor slumping before deposition of the laminated ash.

Lithologic Interpretations

The oldest unit, Unit 5, shows a preponderance of silt-sized vitric ash. The ash is well sorted, lacks coarse fragments, and is thus indicative of wind transportation for some distance. The presence of plant debris, and some grading towards the top of the unit, indicates that the detrital clay and quartz silt were brought in by weak turbidity currents. The beds are distal turbidites, with a considerable addition of tephra. Slump structures indicate that unstable slopes existed at times, possibly due to local channel erosion.

TABLE 2
Unit Descriptions, Depths, Thicknesses, and Ages, Site 297

Unit and Descriptions		Depth (m)	Thickness (m)	Age
1	Diatom/ash rich clay	0-54	54	Late Pleistocene
2	Clay-rich nannofossil ooze	54-90	36	Early-late Pleistocene
3	Claystone	90-330	240	Core 11 (below 206 m) was late Pliocene. No ages given to Core 17 at 395 m.
4	Claystone with interbedded graded silt and sand	330-570	247	Cores 17 and 18 contained early Pliocene fossils
5	Fine vitric ash and ash-rich claystone	570-697.5	122.5	Cores 24-27.contained late early to middle Miocene fossils

Volcanogenic material is negligible in Unit 4, indicating that volcanism probably ceased or waned considerably during the time of deposition. The unit consists of turbidite sequences, clearly shown near the base, with predominant structureless to laminated claystone, which is probably partly turbidite, partly pelagic. Plant debris and detrital quartz indicate a probable continental provenance.

Unit 3 consists of claystone (and some clay), with no plant debris, and only minor volcanogenic silt-sized grains. Volcanism was renewed, but only very fine mainly clay-sized detritus reached the area.

The barren nature of much of Units 3-5, and the poor preservation of the few fossils recovered (apart from those at the base of Unit 5), indicate that the area was below the carbonate compensation depth, except perhaps during the onset of deposition of Unit 5.

The nannofossil ooze of Unit 2 contains early to late Pleistocene foraminifera and nannofossils. Since the area is at present below the supposed local carbonate compensation depth, the presence of such young nannofossil ooze here is puzzling. Several explanations are possible: (1) The site area rose considerably in the late Pleistocene and has since rapidly subsided; (2) A large bloom of nannoplankton enabled deposition to occur below the calcium carbonate compensation depth. However, there is no evidence of corrosion of the fossils such as would be expected in this case; (3) The fossils were brought in by some process (such as turbidity currents) which resulted in rapid deposition and burial. This would not seem likely to result in a fairly pure nannofossil ooze with no obvious signs of reworking; and (4) The calcium carbonate compensation depth at the time of deposition of Unit 2 was for some reason deeper than the present supposed depth.

The preponderance of diatoms in Unit 1 could be the result of a diatom bloom due to favorable conditions, or the selective solution of nannofossils, and dearth of detrital material, resulting in a proportionately greater amount of diatoms. This second condition could occur, for example, if the area was above the calcium carbonate compensation depth during the deposition of Unit 2, but just below it in Unit 1. An added complication in interpreting Units 1 and 2 is that the apparently youngest faunas come from Core 5, in Unit 2. Thus there is a suspicion, either of some disturbance (slumping?) resulting in older sediments overlying younger ones, or that the foraminifera and nannofossils in Unit 1 are all reworked from slightly older Pleistocene deposits, and that no contemporary calcareous fossils survived after deposition of Core 5, because of solution.

PHYSICAL PROPERTIES

Bulk Density, Porosity, and Water Content

Unit 1 (0-54 m), a diatom/ash-rich clay, shows an increase in bulk density, and a corresponding decrease in water content. The physical property plot (Figure 5) shows that a break between Cores 3 and 4 is more appropriate if it was based on density, rather than on lithology. It can be concluded that the changes from the diatom/ash-rich clay (Unit 1) to the clay-rich nannofossil ooze (Unit 2) is gradual rather than abrupt.

Units 2 and 3 (claystone at 54-330 m) are very homogeneous throughout and cannot be separated on physical property data. The change from lithologic Unit 3 to 4 (claystone with some graded silts and sands) between Cores 14 and 15 is one core lower than the physical property data would suggest. Although it was not evident in the cores, it again suggests that the transition is gradual.

Unit 4 (claystone with some graded silts and sands at 330-570 m) shows higher values for density. The wide scattering can be explained by the inhomogeneous nature of this part of the lithologic column. The water-content values follow the same pattern in reverse sense, but scattering is less evident due to fewer sampling points, which are located mainly in the clays.

Unit 5 (fine vitric ash to ash-rich claystone at 570-697.5 m) has a gradual lithologic contact with its overlying unit. According to the physical properties, the boundary between both units should be located below Core 23, rather than above it. This is based on the sharp decrease in density. Within Unit 5, an increase in water content can be observed, which corresponds to the downward increase of clay.

Vane Shear

Units 1, 2, and 3 of Site 297 provided an opportunity to study the variations of shear strength with depth in a hemipelagic sediment. Since shear strength varied with degree of drilling deformation, only the highest values are compiled for a given depth interval. Only vertical measurements (taken from the split core) have been utilized, since the horizontal measurements (taken from the ends of uncut sections) are consistently lower and more erratic. As noted for other sites, the strength data are well ordered above 100 meters and indicate a downhole increase, but show considerable scatter below this level. This scatter is apparently due to drilling deformation and a periodic variation in consolidation observed at depths greater than 100 meters.

It is not immediately apparent why the hemipelagic muds at Site 297 are weaker than the pelagic muds at Sites 294/295 at depths greater than 85 meters. Normally the internal friction of a hemipelagic mud would be higher than a more homogeneous pelagic mud. Since the sedimentation rates of the hemipelagic muds are approximately two orders of magnitude greater than those of the pelagic muds, the former may not have reached an equilibrium state. Given time equivalent to the pelagic muds for physical and chemical diagenesis, the hemipelagic muds would probably be stronger over the entire depth range. The greater shear strength of the pelagic muds may be an artifact of sampling. Further discussion will be found in Bouma and Moore (this volume).

Sonic Velocity and Thermal Conductivity

Sonic velocity and thermal conductivity were measured at least on one section in each of the upper 10 cores. Deeper than Core 11, one section from every even-numbered core was measured. Deeper than Core 20, the sediments were too lithified for needle-probe measurements.

The measured values are tabulated in Tables 3 and 4 and summarized on Figure 6. Estimated thermal conductivities by Ratcliff's formula are also included.

Both sonic velocities and thermal conductivities are fairly uniform in the upper 250 meters. An extremely high sonic velocity at about 160 meters is due to an anomalously lithified layer. Deeper than 300 meters, the thermal conductivity sharply increased to more than 3.6 $\times 10^{-3}$ cal/cm sec°C. This increase corresponds with the remarkable increase in the bulk density in this part (Figure 5).

Unfortunately, measurement of sonic velocity was not made. However, sonic velocity in Core 18 does not deviate from the average trend of increase with depth, while thermal conductivity and bulk density show great anomalies in this core. Therefore, the sonic velocity in this part is estimated not to be far from the general trend of increase.

Heat-Flow Measurements

Two heat-flow measurements were made in situ in the sediment section. The upward heat-flux measurements (Figure 8) were computed from the temperature of the sediments measured at depths of 77 and 253 meters, using the downhole instrument (DHI).

Calculations

The reduction of temperature data has been carried out with the HITAC-10 computer at the Meteorological College of the Japan Meteorological Agency.

TABLE 3
Sonic-Velocity Measurements, Site 297

Sample (Interval in cm)	Depth in Hole (m)	Velocity (km/sec)
3-2, 30.0	21.80	1.507
4-5, 37.0	45.37	1.504
5-5, 37.0	64.37	1.505
6-4, 38.0	81.88	1.599
7-4, 35.0	100.85	1.510
8-3, 30.0	108.80	1.531
9-3, 30.0	127.80	1.497
10-6, 30.0	160.80	1.513
11-3, 30.0	203.80	1.498
11-3, 60.0	204.10	1.505
11-3, 100.0	204.50	1.507
11-3, 120.3	204.70	1.532
12-3, 35.0	251.35	1.560
12-3, 143.0	252.43	1.594
18-2, 115.0	431.15	1.668
22-2, 32.0	553.82	1.879
22-2, 67.0	554.17	1.724
22-4, 50.0	557.00	1.686
23-2, 37.0	591.87	1.993
23-2, 75.0	592.25	1.889
25-4, 47.0	651.97	1.975
25-4, 114.0	652.64	1.942
25-6, 42.0	654.92	1.941
25-6, 97.0	655.47	1.924
26-1, 40.0	666.40	1.851
26-2, 58.0	668.08	2.524
27-1, 31.0	675.81	1.917
27-1, 5.0	675.55	2.122
27-7, 0.0	684.50	2.013

TABLE 4
Thermal Conductivities Measured at Site 297

Sample (Interval in cm)	Hole Depth (m)	Thermal Conductivity in 10^{-3} cal/cm sec°C		
		Needle Probe	Average	From Water Content
3-2, 30	22	1.67		
3-2, 75	22	1.89	1.82	1.95 ±0.11
3-2, 120	22	1.89		
4-5, 40	46	2.27	2.24	2.16 ±0.12
4-5, 110	46	2.20		
5-5, 40	65	1.87		
5-5, 100	65	2.09	2.02	
5-5, 120	65	2.10		
6-4, 40	82	2.03	2.00	2.23 ±0.13
6-4, 110	82	1.97		
7-4, 40	101	2.04	2.01	2.19 ±0.12
7-4, 110	101	2.00		
8-3, 40	109	2.22	2.13	
8-3, 110	109	2.04		
8-5, 144-150	109			2.15 ±0.12
9-3, 40	128	2.19	2.11	2.18 ±0.12
9-3, 110	128	2.03		
10-6, 40	161	2.05	1.98	2.14 ±0.12
10-6, 110	161	1.91		
12-2, 144-150	251			2.19 ±0.12
12-3, 25	251	2.03	1.97	2.21 ±0.12
12-3, 115	251	1.91		
14-5, 40	321	2.61	2.45	
14-5, 110	321	2.28		
14-5, 144-150	321			2.67 ±0.17
16-2, 35	355	3.98		3.52 ±0.25
16-2, 70	355	3.895	3.82	
16-2, 100	355	3.73		
16-2, 125	355	3.19		
18-1, 144-150	355			3.35 ±0.23
18-2, 45	430	3.41	2.98	Hard Contact in watery sand. Omitted from Figure 6.
18-2, 115	430	2.54		

The calculated temperatures show a wide range of variance, which is attributed to the disturbance on thermal probe caused by vertical motions of the drill string due to the pitching of the vessel. These motions could allow two interpretations for the obtained temperature data: first, on an upward motion, the probe would be pulled out of the sediment and exposed to colder circulating water in the hole; secondly, the sudden penetration of the probe into the sediment with a downward motion would cause a heating of the probe, as the probe was gradually getting into thermal equilibrium with the ambient sediment temperature.

The result of these two interpretations are shown in Table 5. In the first interpretation, the maximum value should show the actual in situ temperature of the sediment; in the second interpretation, the minimum values have to show the actual temperature.

If the sea bottom temperature is assumed to be 2°C, then the thermal gradients for the first and second interpretation become 2.33×10^{-3}°C/cm and 1.56×10^{-3}°C/cm, respectively. The thermal conductivity value, 2.03×10^{-3}cal/cm sec °C, is given by averaging the values for upper 77 meters. The heat-flow values obtained are $4.72 \times 10^{-}$cal/cm^{2}sec and $3.17 \times$

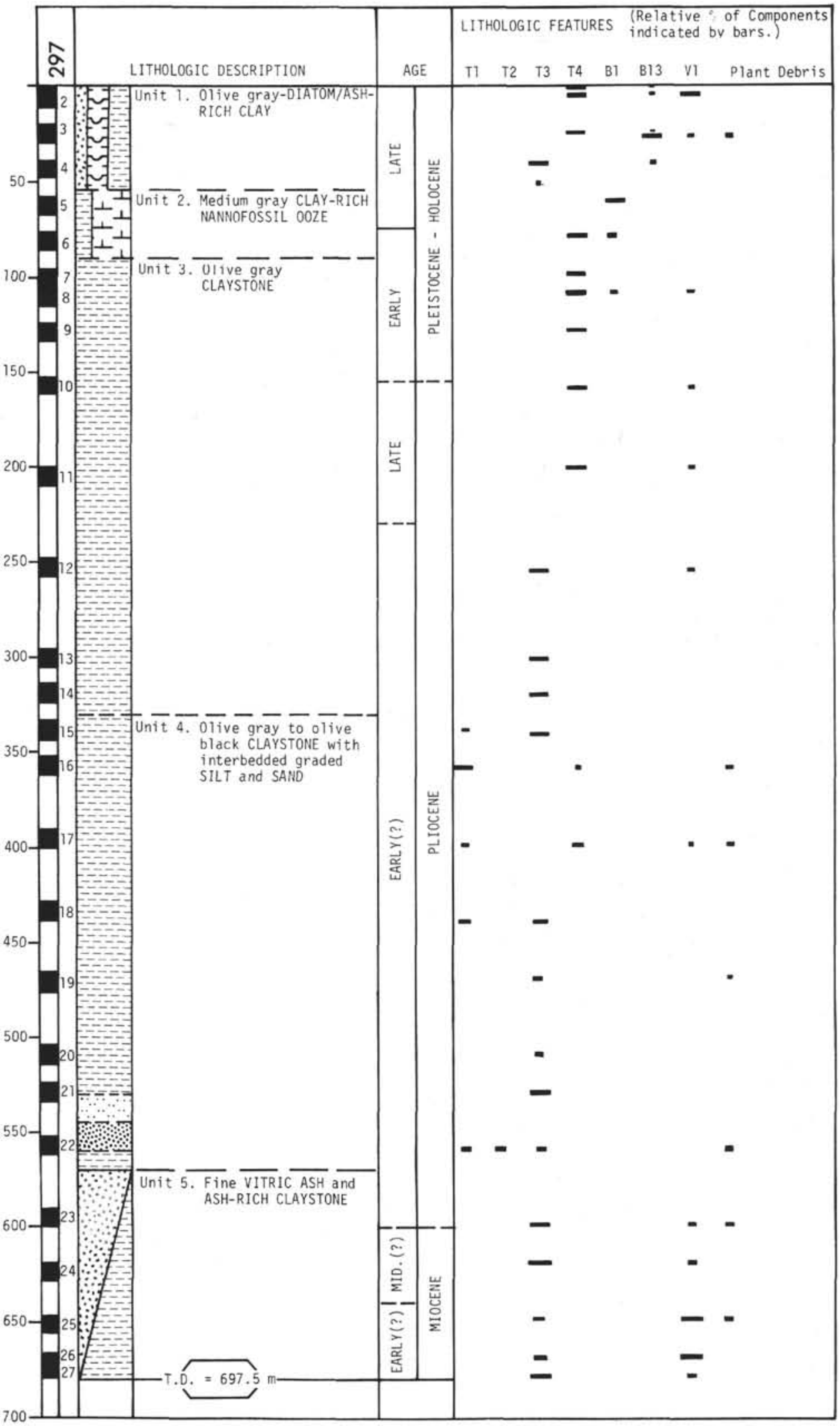

Figure 6. *Lithologic summary – Site 297.*

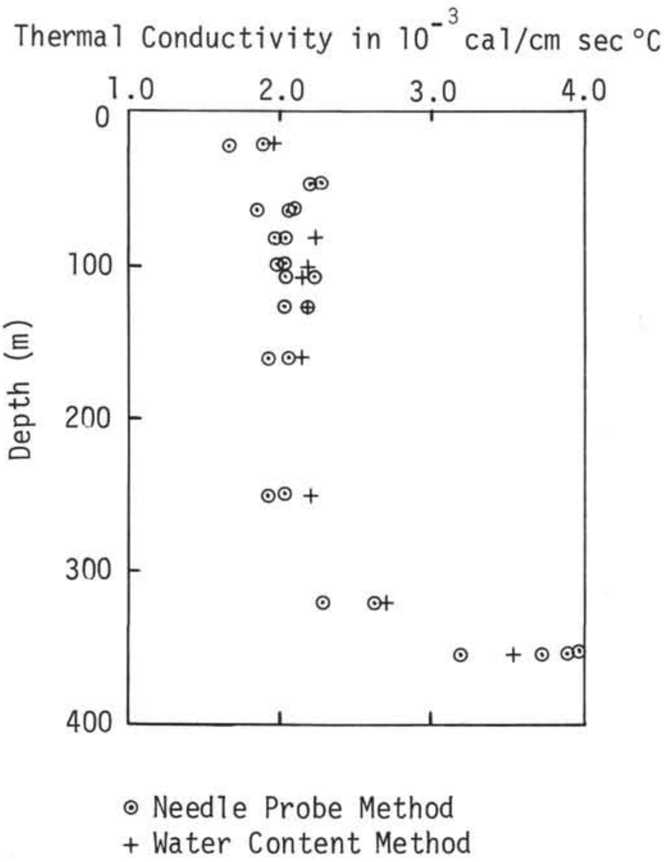

Figure 7. *Thermal-conductivity results, Site 297.*

10^{-6}cal/cm^{2}sec, respectively. These values are remarkably higher than the existing subnormal values (0.75-0.99 × 10^{-6} cal/cm^{2}sec) around this location. This suggests that a narrow, high heat-flow band extends southward from an existing high heat-flow area, located one degree latitude (60 miles) to the north of Site 297.

GEOCHEMICAL MEASUREMENTS

Alkalinity, *p*H, and salinity measurements are summarized in Table 6.

Alkalinity

The average alkalinity of 15 samples examined from Site 297 is 12.19 meq/kg. All of the values are higher than the surface seawater reference value of 2.27 meq/kg. The highest values (greater than 10.0) occur in Cores 3 through 12. The next set of values (Cores 14 through 26) are all below 5.50 meq/kg. The sharp change in alkalinity between Core 12 (14.86) and Core 14 (5.47) is also marked by a lithologic change from an olive-gray claystone in Core 12 to a claystone with interbedded silty sands starting in Core 14.

pH

The average *p*H values in the cores obtained by punch-in and flow-through methods were all below that of the seawater reference at the site (8.20 to 8.19). The 11 punch-in *p*H for Site 297 averaged 7.45, while the 15 flow-through values averaged 7.92. The most noticeable change in *p*H values is that shown by four flow-through values in Cores 14, 22, 24, and 26. These values exceed 8.15, and average 8.32. The high *p*H values correspond to a low alkalinity reported for these cores. The sediments have a dominant claystone lithology.

Salinity

Fifteen salinity measurements at Site 297 averaged 32.7 °/₀₀. A fairly definite decrease in salinity with depth is noticed, except for some variability in Cores 18 and 24. These cores relative to cores above and below from which data were taken contain a high percentage of sand, silt, and ash interbeds, within a claystone lithology. All 15 values and their average were below the overlying seawater reference value of 34.4°/₀₀.

PALEONTOLOGIC SUMMARY

Introduction

Pleistocene through early Miocene microfossils are present at Site 297, with siliceous and calcareous forms occurring in moderate to high abundances throughout the sequence. Preservation of all groups is moderate to

TABLE 5
Heat-Flow Measurements, Site 297

	First Interpretation[a]				Second Interpretation[a]			
Depth (m)	Temperature (°C)	Thermal Gradient (10^{-3}°C/cm)	Thermal Conductivity (10^{-3} cal/ cm sec°C)	Heat Flux (10^{-6} cal/cm^{2}sec)	Temperature (°C)	Thermal Gradient (10^{-3}°C/cm)	Thermal Conductivity (10^{-3} cal/ cm sec°C)	Heat Flux (10^{-6} cal/cm^{2}sec)
0[b]	2	2.33	2.03	4.72		1.56	2.03	3.17
77	20.0				14.0			

[a] See text.

[b] Assumed bottom-water temperature.

TABLE 6
Summary of Shipboard Geochemical Data, Site 297

Sample (Interval in cm)	Depth Below Sea Floor (m)	*p*H		Alkalinity (meq/kg)	Salinity (°/₀₀)	Lithologic Unit
		Punch-in	Flow through			
Surface seawater reference		8.20	8.19	2.27	34.4	
3-1, 144-150	21.5	7.57	7.73	17.79	34.4	Unit 1
5-4, 144-150	64.0	7.30	7.58	21.41	33.8	Unit 2
6-5, 144-150	84.5	7.70	8.15	23.17	33.6	
8-5, 144-150	113.0	7.28	7.84	23.07	33.3	Unit 3
10-5, 144-150	160.5	7.49	7.90	22.58	33.0	
11-3, 144-150	205.0	7.19	7.77	17.79	32.7	
12-2, 144-150	251.0	7.35	7.73	14.86	32.7	
14-5, 144-150	322.0	7.64	8.22	5.47	31.9	
17-2, 144-150	393.5	7.67	7.94	6.94	32.2	Unit 4
18-1, 144-150	430.0	7.62	7.62	4.89	33.3	
20-2, 144-150	507.5	7.20	7.41	6.35	32.2	
22-3, 144-150	536.5	–	8.19	4.59	31.9	
23-3, 144-150	594.5	–	7.82	6.16	30.0	Unit 5
24-1, 144-150	620.0	–	8.30	5.08	33.0	
26-1, 0-4	666.0	–	8.56	2.64	31.9	
Average		7.45	7.92	12.19	32.7	

good. Planktonic foraminifera, calcareous nannofossils, radiolarians, diatoms, and silicoflagellates were used to recognize Pleistocene sediments, whereas only planktonic foraminifera and nannofossils were used in recognizing middle and early Miocene sediments.

Calcareous nannofossil and foraminiferal zonations indicate that the sediments within Cores 1 through 11 (0-205 m) are Pleistocene in age. However, the stratigraphic order within this portion of the section is not straightforward. Curiously, there is an occurrence of clearly latest Pleistocene/Holocene calcareous nannofossils and planktonic foraminifera, out-of-sequence beneath late Pleistocene material within Core 4, Section 6 through Core 5 (48-67.5 m). More specifically, the late Pleistocene *Gephyrocapsa oceanica* Zone occurs in Cores 1 through 4, Section 4, with the younger *Emiliania huxleyi* Zone beneath it in Cores 4 and 5. The only possible explanation of this our-of-order sequence appears to be downhole slumping.

Core 11 (200.5-210.0 m) contains late Pliocene foraminifera and calcareous nannofossils, with an arbitrary Pleistocene-Pliocene boundary drawn at the base of Core 10 (162.5 m). Cores 11 through 15 (257-343 m) are essentially barren of fossils, except for a few reworked shallow-water benthonic foraminifera. However, Core 16 (352.5-362.0 m) contains sparse early Pliocene planktonic foraminifera, including *Globigerina nepenthes.* Core 17 (395.5-400.0 m) contains non-diagnostic calcareous nannofossils, along with displaced shallow-water benthonic foraminifera and reworked middle Miocene planktonic foraminifera. Core 18 (428.5-438 m) contains both early Pliocene planktonic foraminifera and nannofossils.

Unfortunately, Cores 19 through 23 (476-599 m) are completely barren of microfossils. However, Cores 24 through 27 (628-679 m) contain middle to late early Miocene planktonic foraminifera, nannofossils, radiolarians, and diatoms.

Calcareous Nannofossils

The generally poor state of preservation and paucity of nannofossils except for the youngest, and possibly the oldest samples, suggest that deposition occurred at or below the carbonate compensation depth. Several scattered nannofossils were recovered from the silty fraction of the turbidite sequence because they probably were preserved by rapid burial.

Samples from Cores 1 through 4, Section 4 contain specimens characteristic of the late Pleistocene *Gephyrocapsa oceanica* Zone. A floral assemblage of the Holocene-late Pleistocene *Emiliania huxleyi* Zone was recovered from Core 4, Section 6 through Core 5. The nannofossil assemblage from this sample interval appears to occur out of sequence; however, the occurrence of specimens of *E. huxleyi* in samples from Cores 1 through 4, Section 4 may have been in such low abundance that it escaped detection. If this were the case, then the first three core samples would also belong to the *E. huxleyi* Zone. Nevertheless, these uppermost samples lack many of the nannofossils found in association with *E. huxleyi* in the samples from Core 4, Section 6 through Core 5.

Samples from Cores 6 through 11, Section 3 contain specimens of the early Pleistocene *Gephyrocapsa caribbeanica* Subzone. The sample from Core 11, Section 4 contains abundant *Emiliania ovata* and common *E. annula,* which may be indicative of the early Pleistocene *Emiliania annula* Subzone.

Sample 11, CC contains abundant, well-preserved specimens of the youngest Pliocene *Cyclococcolithina macintyrei* Subzone. Cores 12 through 16 are essentially barren, with only a few etched or overgrown unidentifiable specimens present. Core 17 contains only a few rare, poorly preserved reworked specimens of Eocene-Oligocene and Miocene-Recent age and cannot be placed in an age framework. The sample from Core 18 contains a fair abundance of late early Pliocene nannofossils that can best be referred to the *Reticulofenestra pseudoumbilica* Zone. Although poorly preserved, these specimens are probably indigenous to the sediment in which they occur. Cores 19 through 23 are essentially barren, with only a few unidentifiable nannofossils fragments.

Samples from Core 24 contain a mixed assemblage of predominantly discoasters that can probably best be placed in the middle Miocene. Succeeding samples from Cores 25 and 26 contain a few, poorly preserved nannofossils that do not have any age significance. Relatively well-preserved nannofossils occur rather commonly in the Core 27 sample. Although a few reworked Eocene specimens are present, the fairly diverse assemblage clearly identifies the middle Miocene *Sphenolithus heteromorphus* Zone.

Foraminifera

Foraminifera are generally limited in their major occurrence to the upper muddy sediments (Cores 1 through 11). As the lithology becomes sandy below Core 12, no foraminifera were recovered, except for rare to a few reworked specimens in the interval between Cores 15 and 19.

The age assignment of the upper horizons is based mainly on the relationship of the *Globorotalia truncatulinoides-G. tosaensis* lineage, along with the appearance of *Pulleniatina obliquiloculata finalis*. These assemblages are similar to those of the Pleistocene to upper Pliocene interval at Site 296.

An interesting, and as yet not fully understood inconsistency is noted for the age of Core 5, in relation to the samples of Cores 1 to 3. While the upper three samples yield a significant number of specimens of *G. tosaensis* together with that of *G. truncatulinoides* suggesting an early Pleistocene (lower N22) age, Core 5 contains abundant specimens of typical *G. truncatulinoides*, indicating a late Pleistocene to Holocene (upper N22 to N23) age. This reversal of age agrees with that noticed by nannofossils. Consequently, the interval above Core 5 may represent reworked or displaced sediments. This assumption is supported by the occurrence of comparatively fewer specimens of calcareous foraminifera, and by their good preservation, despite the fact that the water depth at this site is below the present calcium carbonate compensation depth.

Foraminifera from Cores 15 to 19 are so rare that they were recovered only after flotation by measn of dibromethane liquid. These faunas can be divided into two different assemblages based upon this state of preservation; a reworked fauna, in which all individuals were stained a deep brownish color, and another representing a displaced fauna with a younger appearance but always containing shallow-water elements such as *Ammonia inflata*, *A. japonica*, *A. beccarii* var., *Pararotalia nipponica*, *Buccella frigida*, *Cibicides cushmani*, some Quinqueloculines, and Triloculines. All of these latter species typically occur in the neritic environment off Shikoku Island. The ages suggested by these displaced faunas may be approximately that of the sediments containing them; Core 17 is assigned to the early Pliocene (probably N19), and Core 18 to the early early Pliocene (N18). However, Core 16 contains a reworked planktonic fauna of early Pliocene age, and Core 17 contains a reworked middle Miocene planktonic assemblage.

Radiolarians and Silicoflagellates

A rich and well-preserved Pleistocene radiolarian assemblage is found from Cores 1 through 5 (0-67.5 m). However, they are completely absent in Cores 6 through 25. A few radiolarians are observed from Sample 26-2, 140-143 cm and fine sandy portion of Core Catcher 26 is assigned to the *Calocycletta costata* Zone. Radiolarians are completely absent in the fine silty clayey portions of Cores 26 and 27.

The silicoflagellates *Dictyocha fibula*, and its varieties, *D. f.* var. *aculeata* and *D. f.* var. *messanensis*, were recovered from the Pleistocene interval (Cores 1 through 6). This group of microfossils is completely absent below Core 7, to the bottom of the hole in Core 27.

Diatoms

The following Quaternary diatoms occur commonly in Cores 1 through 5: *Coscinodiscus lineatus*, *C. nodulifer*, *Nitzschia marina*, *Pseudoeunotia doliolus*, and *Rhizosolenia bergonii*, which all belong to the *Pseudoeunotia doliolus* Zone (Pleistocene-Recent) of Burckle (1972). In addition, some sublittoral species *Actinocyclus ehrenbergii*, *Actinoptychus undulatus*, *Cocconeis scutellum*, *Diploneis bombus*, *D. suborbicularis*, and *Grammatophora oceanica* were also found. The freshwater species *Cyclotella* sp., *Cymbella* sp., *Eunotia* sp., and *Melosira granulata* were also encountered in Cores 2 and 3.

Although *Thalassiosira convexa*, a Pliocene index species, is found together with *Coscinodiscus africanus*, *Nitzschia reinholdii*, and *Rhizosolenia bergonii*, and fresh-water species in Core 6, another Pliocene index species, *Rhizosolenia praebergonii*, is absent. Only freshwater and sublittoral species are found in Core 9. Many fragments of frustules of *Kieselavia carina*, an index species of late early to middle Miocene age, are encountered in Core 25. A few fragments of diatom valves are occasionally observed in samples from Cores 7 through 27.

SUMMARY AND INTERPRETATIONS

Summary

Equipment failures limited the depth of the hole to 679.5 meters and prevented the penetration of the entire stratigraphic section at Site 297. However, there is sufficient control to estimate a total sediment cover of about 800 meters. The section can be divided into four major units on the basis of sedimentological and seismic reflection characteristics.

1) Upper Transparent Layer
   Unit 1 (0-54 m) diatom ash-rich clay; late Pleistocene
   Unit 2 (54-90 m) clay-rich nannofossil ooze; Pleistocene
   Unit 3 (90-330 m) claystone; late Pliocene-Pleistocene

2) Middle Reflective Layer
   Unit 4 (330-570 m) terrigenous turbidites; late Miocene-early Pliocene
3) Lower Moderately Transparent Layer
   Unit 5 (570-800 m) volcanic-rich clay; early to late Miocene
4) Opaque Acoustic Basement

Interpretation

Although a primary objective of investigating the basement was negated, there are strong indications that the opaque acoustic basement reflector at 0.83 sec represents basalt. The several hundred meter relief of this reflector in the site area (Figure 2), and its known ridge-trough nature in other sections of the basin (Karig, this volume), are analogous to that of demonstrable basaltic basements in other marginal basins (Karig, 1971a, b; Sclater et al., 1972). A further indication that this basement consists of basalt rather than of faulted sediments is found in its high (5.1 km/sec) compression velocity (Yoshii et al., 1973).

The extrapolated depth of 100 meters from the base of Hole 297 to this basement is relatively insensitive to the seismic velocity assumed. However, the value of 2.2 km/sec used is based on shipboard sonic measurements on samples from Site 297, adjusted to in situ conditions. Sedimentation rates above the last core are about 22 m/m.y., and the downward increase in ash and biogenous content suggests that the rate in the bottommost interval is at least as high. Unless there is a sedimentary hiatus, for which there is no sign on reflection profiles, it is almost impossible to project an age for basement other than very early Miocene. That this mid-Tertiary acoustic basement represents the initial basin crust is supported by the moderately high heat flow (Watanabe et al., 1970; Sclater, 1972; and others); the increase in carbonate content toward the base of the section in Hole 297: and the thin crust delineated by refraction measurements (Murauchi et al., 1968, Yoshii et al., 1973).

Site 297 lies approximately halfway between the Palau-Kyushu Ridge and a line of rough topography running down the center of the Shikoku Basin, which appears to mark the final position of the spreading zone (Karig, this volume). The duration of the extension in the Shikoku Basin apparently extends from the very late Oligocene well into the early Miocene (Karig, this volume), indicating that the Shikoku and Parece Vela basins opened simultaneously and were part of a single large marginal basin.

The Shikoku Basin has a thick sediment cover compared to the rest of the Philippine Sea. This is because of its proximity to Japan and because there apparently was no trench along the basin-flanking margin southwest Japan throughout most of the basin history. This sediment cover varies from almost 1000 meters at the northwest corner of the basin to approximately 800 meters at the northeast corner. It thins southward to merge with the thin pelagic cover of the Parece Vela Basin near 25°N. In the northwestern part of the Shikoku Basin, the sediment cover can be divided into the three acoustic units recognized at Site 297.

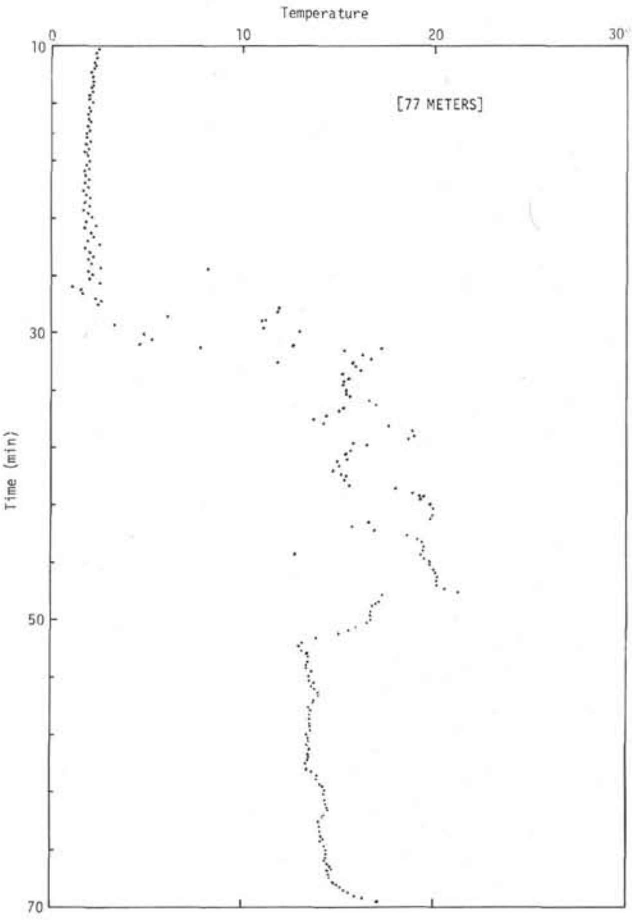

Figure 8. *Heat-flow results, Site 297.*

The hemipelagic nature and northern source of the upper transparent unit are demonstrated by its slow southward thinning over a distance of several hundred kilometers and by its pelagic geometry, especially at the southern part of its range. The volcanic ash of the uppermost part of this unit must be derived from Kyushu, some 300 km to the northwest, as there has been no volcanic activity in Japan opposite the Shikoku Basin, and the current and wind direction would not easily allow Bonin arc debris to be transported westerly.

The lower two acoustic units in the northwestern Shikoku Basin, the reflective turbidite sequence and the basal semitransparent ash and claystone, thin more rapidly southward and cannot be identified more than 150 km south of the trench. This transition from hemipelagic to turbiditic deposition in the late Miocene (?) may mark uplift of southwest Japan, perhaps as an early manifestation of a subduction pulse.

Turbidite deposition terminated in the Pliocene (3 m.y.) when the Nankai Trough developed sufficiently to trap these terrigenous sediments. The rapid deposition of pelagic to hemipelagic sediment in the northern Shikoku Basin, following the development of the Nankai Trough, must be attributed to an efficient transport of clay-sized particles from Japan through the air or water column, and to a large contribution of biogenous and volcanic material.

The present water depth (4458 m) at Site 297 is well below the regional carbonate compensation depth (CCD), and yet calcareous microfossils are abundant in portions of the Pleistocene section and are common in early to mid-Miocene sediments. The lower calcareous section can be related to the basin initiation, when water depths were less than the CCD.

The presence of well-preserved calcareous and siliceous fossils (including diatoms) in the early Miocene and earliest mid-Miocene interval at the base of Hole 297 suggests that the depth of this portion of the basin was above the CCD during the initial stages of its formation. The approximate boundary between the oldest sediments containing calcareous planktonic remains and those barren of these microfossils is present at 620 meters suggesting subsidence to a depth in excess of 4000 meters by early mid-Miocene time. This interpretaion is corroborated in part by the fact that the overlying sequence of almost 400 meters of mid-Miocene through early Pleistocene sediments are essentially barren of fossils with the exception of rare and poorly preserved shallow-water benthonic foraminifera and rare early Pliocene planktonic fossils preserved due to rapid burial in turbidite horizons.

In contrast to the lengthy interval of carbonate-poor sediment, a late Pleistocene calcareous nannofossil ooze is present at 54 to 90 meters with planktonic foraminifera also present in younger overlying sediment. Several recent studies (Kent et al., 1971; Hays et al., 1969; Ingle, 1973) of Pleistocene climatic events in the North Pacific have found substantial evidence of a major climatic cooling beginning about 700,000[2] years B.P. which is now recognized as the initiation of the so-called glacial Pleistocene. It is reasonable to expect that such an event would be expressed in mid-latitude areas of major boundary currents as a period of increased surface circulation and overturn leading to a prolific rain of planktonic debris in the affected areas. The late Pleistocene nannofossil ooze and other calcareous planktonic fossils of this age present at Site 297 are thus interpreted as a manifestation of increased productivity within the Kuroshio Current during the glacial Pleistocene.

Rapid accumulation of planktonic tests, in effect, overwhelmed and effectively depressed the CCD within this portion of the Shikoku Basin during the major period of climatically intensified surface circulation during the late Pleistocene. A decrease in climatic gradient during the past 12,000 years, and for short intervals during the preceding 700,000 years, should be expressed by a decrease in calcareous debris with a concomitant relative increase of siliceous plankton such as seen in Cores 1 to 4 (0-48.5 m).

REFERENCES

Berggren, W., 1972. A Cenozoic time-scale—some implications for regional geology and paleobiogeography: Lethaia, v. 5, p. 195-215.

Burckle, L. H., 1972. Late Cenozoic planktonic diatom zones from the eastern Equatorial Pacific: Beih. Nova Hed., Heft 39, p. 217-246.

Chase, T. E., Menard, H. W., et al., 1969. Bathymetric atlas of the Northwestern Pacific: Washington (U.S. Oceanographic Off. Hq., Publ. 1301).

Fischer, A. G., et al., 1971. Initial Reports of the Deep Sea Drilling Project, Volume 6: Washington (U.S. Government Printing Office).

Fitch, T. J. and Scholz, C. H., 1971. Mechanism of underthrusting in southwest Japan: a model of convergent plate interactions: J. Geophy. Res., v. 76, p. 7260-7292.

Hays, J. D., Saito, T., Opdyke, N., and Burckle, L., 1969. Pliocene-Pleistocene sediments of the equatorial Pacific: their paleomagnetic, biostratigraphic, and climatic record: Geol. Soc. Am. Bull., v. 80, p. 1481-1514.

Hilde, T. W. C., Wageman, J. M., and Hammond, W. T., 1969. The structure of Tosa Terrace and Nankai Trough off southeastern Japan: Deep Sea Res., v. 16, p. 67-75.

Ingle, J. C., Jr., 1973. Neogene foraminifera from the northeastern Pacific; Leg 18. *In* Kulm, L. D., von Huene, R., et al., Initial Reports of the Deep Sea Drilling Project, Volume 18: Washington (U.S. Government Printing Office), p. 517-568.

Kanimori, H., 1972. Tectonic implications of the 1944 Tonankai and the 1946 Nankaido earthquakes: Phys. Earth Planet. Interiors, v. 5, p. 129-139.

Karig, D. E., 1971a. Origin and development of marginal basins in the western Pacific: J. Geophy. Res., v. 76, p. 2542-2560.

________, 1971b. Structural history of the Mariana Island Arc system: Geol. Soc. Am. Bull., v. 82, p. 323-344.

Kent, D., Opdyke, N. D., and Ewing, M., 1971. Climatic change in the North Pacific using ice-rafted detritus as a climatic indicator: Geol. Soc. Am. Bull., v. 82, p. 2741-2754.

Murauchi, S., Den, N., Asano, S., Hotta, H., Yoshii, T., Asanuma, T., Hagiwara, K., Ichikawa, K., Sato, T., Ludwig, W. J., Ewing, J. I., Edgar, N. T., and Houtz, R. E., 1968. Crustal structure of the Philippine Sea: Tectonophysics, v. 10, p. 3143-3171.

Sclater, J. G., 1972. Heat flow and elevation of the marginal basins of the Western Pacific: J. Geophys. Res., v. 77, p. 5705-5719.

Sclater, J. G., Hawkins, J. W., Jr., Mammerickx, J., and Chase, C. G., 1972. Crustal extension between the Tonga and Lau ridges; petrologic and geophysical evidence: Geol. Soc. Am. Bull., v. 83, p. 505-518.

Watanabe, T., Epp, D., Uyeda, S., Langseth, M., and Yasui, M., 1970. Heat flow in the Philippine Sea: Tectonophysics, v. 10, p. 205-224.

Yoshii, T., Ludwig, W. J., Dean, N., Nurauchi, S., Ewing, M., Hotta, H., Buhl, P., Asanuma, T., and Sakajii, N., 1973. Structure of southwest Japan margin off Shikoku: J. Geophys. Res., v. 78, p. 2517-2525.

---

[2] Or alternately 900,000 years B.P., depending on interpretation of associated paleomagnetic stratigraphy.

APPENDIX A
Summary of X-Ray, Grain Size, and Carbon-Carbonate Results, Site 297

Section	Sample Depth Below Sea Floor (m)	Lithology	Age	Bulk Sample Major Constituent			2-20μm Fraction Major Constituent			<2μm Fraction Major Constituent			Grain Size			Classification	Carbon Carbonate			Comments
				1	2	3	1	2	3	1	2	3	Sand (%)	Silt (%)	Clay (%)		Total (%)	Organic (%)	$CaCO_3$ (%)	
297-3-1	21.1	Unit 1 Diatom-ash-rich clay	Late Pleistocene	Quar.	Mica	Plag.	Quar.	Plag.	Mica	Mica	Quar.	Plag.	0.4	39.6	60.0	Silty clay	0.4	0.3	1	
297-4-3	42.8			Quar.	Mica	Plag.	Quar.	Plag.	Mica	Mica	Quar.	Mont.	0.1	48.6	51.2	Silty clay	0.7	0.5	1	Pyrite in <2μm (2.7%)
297-5-4	63.3	Unit 2 Clay-rich nannofossil ooze	Early to late Pleistocene										0.4	34.3	65.3	Silty clay	2.3	0.5	15	
297-5-5	64.4			Quar.	Mica	Calc.	Quar.	Plag.	Mica	Mica	Quar.	Mont.								
297-6-5	83.8			Quar.	Mica	Plag.	Quar.	Plag.	Mica	Mica	Quar.	Plag.					1.2	0.4	7	
297-7-3	100.3	Unit 3 Claystone	Late Pliocene (below 206 m)														0.7	0.4	2	
297-8-5	112.3												0.1	38.0	61.9	Silty clay	0.8	0.4	3	
297-12-2	250.2			Quar.	Mica	Plag.	Quar.	Mica	Plag.	Mica	Quar.	Mont.	0.4	41.7	57.8	Silty clay				
297-13-1	296.9												0.1	38.7	61.2	Silty clay				
297-14-4	319.7			Mica	Quar.	Plag.	Quar.	Plag.	Mica	Quar.	Mica	Mont.	0.1	31.6	68.3	Silty clay				
297-15-4	338.7	Unit 4 Claystone with interbedded graded silt and sand	Early Pliocene (Cores 17 and 18)										0.2	28.6	71.2	Silty clay				
297-18-2	430.8												10.2	68.8	21.0	Clayey silt				
297-19-1	467.5												2.0	56.8	41.2	Clayey silt				
297-19-1	467.8												56.2	28.4	15.4	Silty sand				
297-22-2	554.3												28.9	46.4	24.7	Sand-silt-clay				
297-22-3	555.5												0.3	76.1	23.7	Silt				
297-22-4	556.8												3.1	73.5	23.4	Clayey silt				
297-24-3	622.3	Unit 5 Fine vitric ash and ash-rich claystone	Late early to middle Miocene	Mont.	Quar.	Mica	Quar.	Plag.	Mica	Mont.	Mica	Quar.	0.3	52.9	46.7	Clayey silt				
297-26-1	666.0												0.0	53.5	46.5	Clayey silt				
297-26-2	668.8			Quar.	Mica	Mont.	Quar.	Mica	Plag.	Mont.	Quar.	Mica								

Note: Complete results of X-ray, Site 297, will be found in Part V, Appendix I. X-ray mineralogical legend on Appendix A, Chapter 2.

Site 297 Hole Core 1 Cored Interval: 0.0-1.0 m

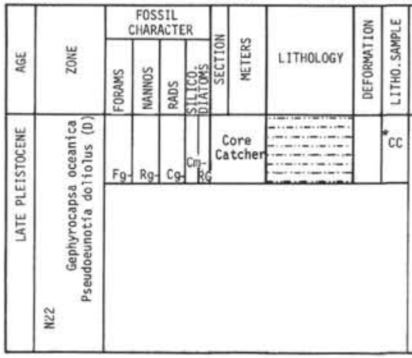

LITHOLOGIC DESCRIPTION

UNIT 1
5GY 4/1

SILTY CLAY (DIATOM RICH)
Smear: CC

Texture	Composition
47% Clay	40% Clay minerals
40% Silt	15% Diatoms
3% Sand	10% Radiolarians
	8% Feldspar
	7% Quartz
	6% Sponge spicules
	5% Heavy minerals
	3% Volcanic glass
	3% Pyrite
	2% Micarb
	1% Nannofossils

Explanatory notes in chapter 1

Site 297 Hole Core 2 Cored Interval: 1.0-10.5 m

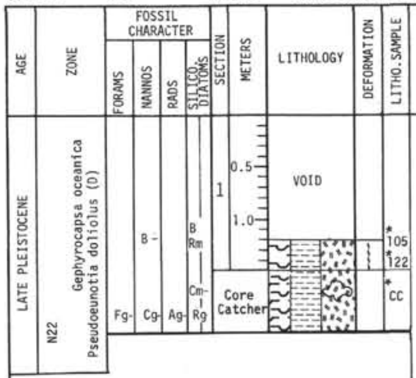

LITHOLOGIC DESCRIPTION

10YR 6/2 &
5Y 4/1

Olive gray (5Y 4/1); intense drilling deformation; pale yellow brown (10YR 6/2) ash plus green gray (5GY 6/1) colors.

DIATOM-RICH CLAYEY ASH
Smears: 1-122, 1-105, CC

Texture	Composition
55% Clay	40% Volcanic glass
45% Silt	21-31% Clay minerals
	14-15% Diatoms
	10% Feldspar
	2% Heavy minerals
	2% Micarb
	2% Sponge spicules
	1% Nannofossils
	Tr% Radiolarians

VOLCANIC ASH
Smear: CC

Composition
89% Volcanic glass
5% Clay minerals
3% Feldspar
1% Heavy minerals
1% Micarb
1% Diatoms

Explanatory notes in chapter 1

Site 297 Hole Core 3 Cored Interval: 20.0-29.5 m

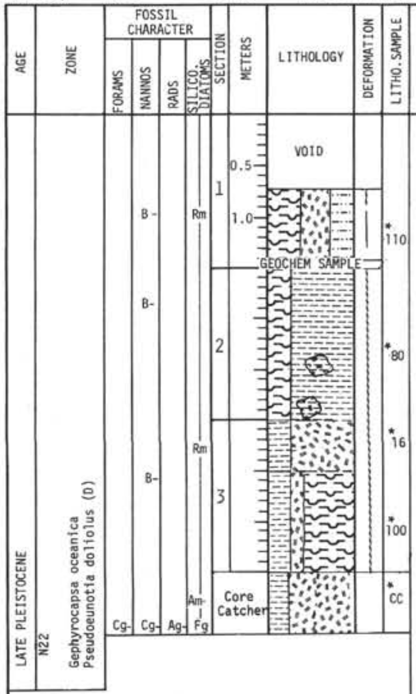

LITHOLOGIC DESCRIPTION

5Y 4/1

Color dominant olive gray (5Y 4/1; soft-stiff. Intense drilling deformation; some peat(?) fragments in core catcher.

DIATOMACEOUS ASHY SILTY CLAY
Smear: 1-110

Texture	Composition
60% Clay	30% Clay minerals
40% Silt	30% Diatoms
	27% Volcanic glass
	5% Radiolarians
	4% Feldspar
	2% Heavy minerals
	1% Micarb
	1% Silicoflagellates
	Tr% Nannofossils

DIATOM-RICH CLAY
Smear: 2-80

Composition
77% Clay minerals
10% Diatoms
5% Volcanic glass
4% Feldspar
3% Radiolarians
1% Heavy minerals
Tr% Sponge spicules
Tr% Silicoflagellates

CLAY-RICH ASH
Smears: 3-16, CC

Composition
69-81% Volcanic glass
10-15% Clay minerals
5- 8% Diatoms
3% Feldspar
1- 2% Heavy minerals
Tr- 1% Micarb
Tr% Nannofossils
Tr% Sponge spicules

ASH/CLAY-RICH DIATOM OOZE
Smear: 3-100

Composition
44% Diatoms
20% Volcanic glass
10% Micronodules
10% Clay minerals
8% Feldspar
6% Heavy minerals
1% Micarb
1% Radiolarians

Grain Size 1-107	Carbon Carbonate 1-111
0.4, 39.6, 60.0	0.4, 0.31 1

X-ray 1-109 (Bulk)
41.9% Quar
28.5% Mica
22.1% Plag
5.7% Chlo
1.8% Mont

Explanatory notes in chapter 1

Site 297 Hole Core 4 Cored Interval: 39.0-48.5 m

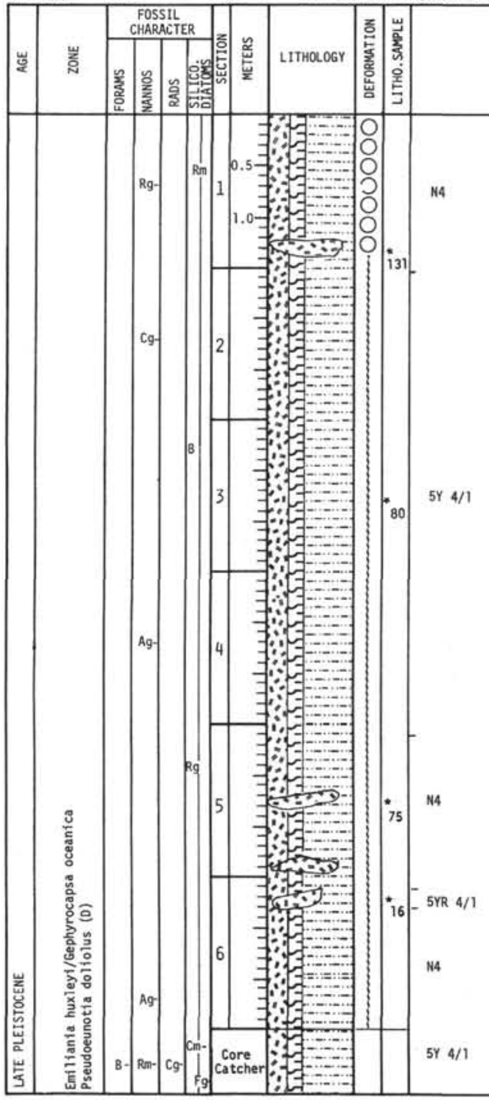

LITHOLOGIC DESCRIPTION

Color basically medium dark gray (N4), brown gray (5YR 4/1), olive gray (5Y 4/1); deformation - intense to breccia.

ASH/DIATOM-RICH SILTY CLAY
Smears: 3-80, 5-75

Texture	Composition
51% Clay	61-68% Clay minerals
49% Silt	10-15% Diatoms
	10-13% Volcanic glass
	5% Feldspar
	2% Heavy minerals
	Tr- 5% Radiolarians
	Tr% Sponge spicules

VOLCANIC ASH
Smears: 1-131, 6-16

Texture	Composition
40% Sand	63-96% Volcanic glass
30% Silt	20% Clay minerals
30% Clay	5% Feldspar
	3-12% Heavy minerals
	1% Micarb
	Tr% Diatoms

Grain Size 3-77
0.1, 48.6, 51.2

Carbon Carbonate 3-81
0.7, 0.5, 1

X-ray 3-79 (Bulk)
40.7% Quar
32.5% Mica
18.8% Plag
5.2% Chlo
2.8% Mont

Explanatory notes in chapter 1

Site 297 Hole Core 5 Cored Interval: 58.0-67.5 m

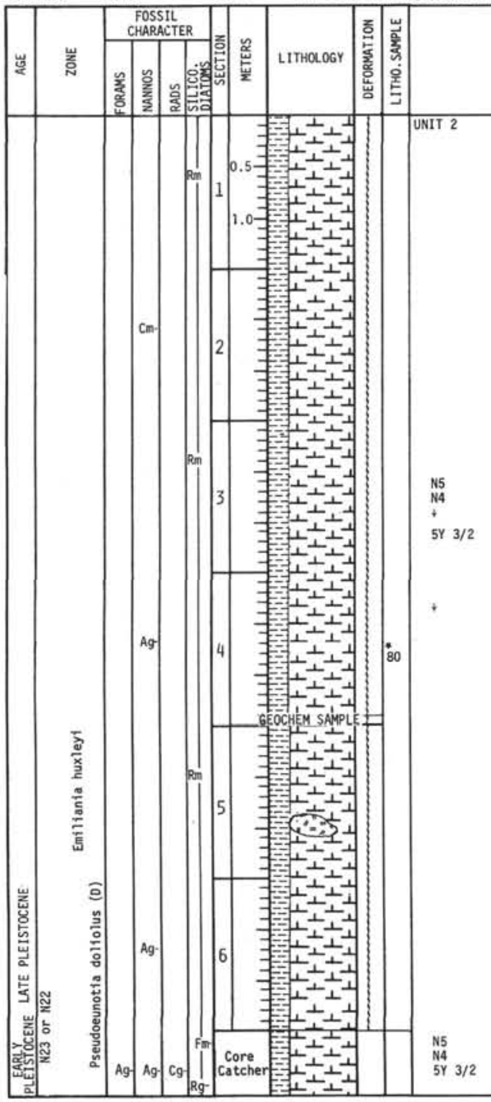

LITHOLOGIC DESCRIPTION

Colors medium gray (N5) to medium dark gray (N4) with olive gray 5Y 3/2; intense drilling deformation - soft.

CLAY-RICH NANNOFOSSIL OOZE
Smear: 4-80

Texture	Composition
65% Clay	63-66% Nannofossils
34% Silt	20% Clay minerals
0- 1% Sand	3- 6% Volcanic glass
	5% Feldspar
	2% Heavy minerals
	2% Micarb
	1% Radiolarians
	1% Diatoms
	Tr% Foraminifera
	Tr% Sponge spicules

Grain Size 4-78
0.4, 34.3, 65.3

Carbon Carbonate 4-80
2.3, 0.5, 15

X-ray 5-41 (Bulk)
33.0% Quar
25.4% Mica
18.6% Calc
16.3% Plag
3.7% Chlo
3.1% Mont

Explanatory notes in chapter 1

Site 297 Hole Core 6 Cored Interval: 77.0-86.5 m

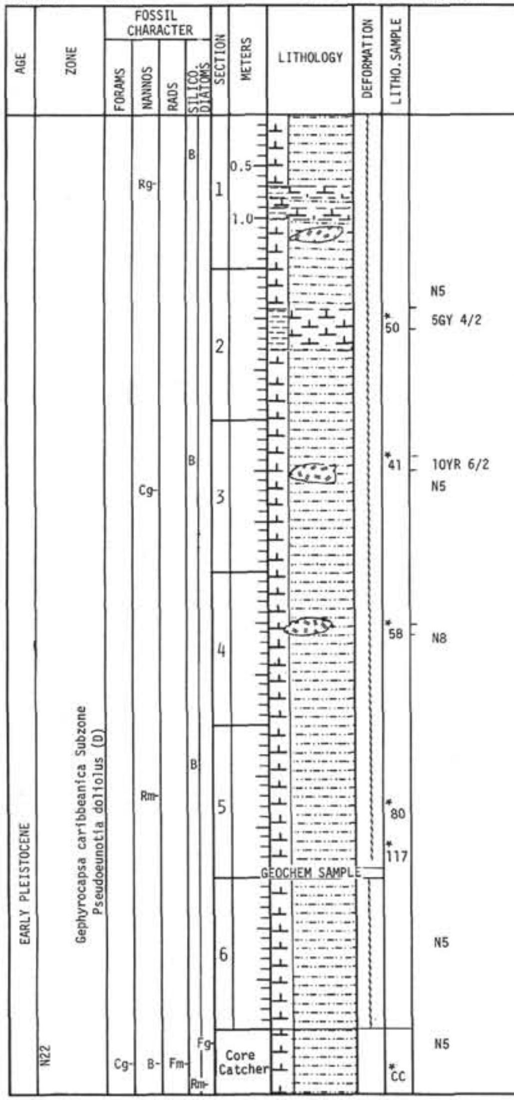

LITHOLOGIC DESCRIPTION

Color mainly medium gray (N5) with streaks of dark gray purple (5P 3/2) - dark dusky yellow green streaks (5GY 4/2). Intense drilling deformation.

NANNOFOSSIL-RICH SILTY CLAY
Smears: 5-80, 5-117, CC

Texture	Composition
60% Clay	68-70% Clay minerals
40% Silt	0-10% Nannofossils
	5-10% Feldspar
	3% Volcanic glass
	2% Heavy minerals
	2% Zeolite
	0-1% Diatoms
	Tr% Foraminifera
	Tr% Radiolarians

CLAY-RICH NANNOFOSSIL OOZE
Smear: 2-50

Composition
72% Nannofossils
15% Clay minerals
5% Volcanic glass
3% Feldspar
2% Micarb
2% Radiolarians
1% Heavy minerals
Tr% Diatoms
Tr% Sponge spicules

VOLCANIC ASH
Smears: 3-41, 4-58

Texture	Composition
40-60% Silt	79-94% Volcanic glass
15-50% Sand	3-10% Feldspar
10-25% Clay	3% Micarb
	0-10% Clay minerals
	Tr- 1% Heavy minerals

Carbon Carbonate 5-82
1.2, 0.4, 7

X-ray 5-79 (Bulk)
34.8% Quar
35.8% Mica
20.5% Plag
10.9% Calc
4.2% Chlo
3.8% Mont

Explanatory notes in chapter 1

Site 297 Hole Core 7 Cored Interval: 96.0-105.5 m

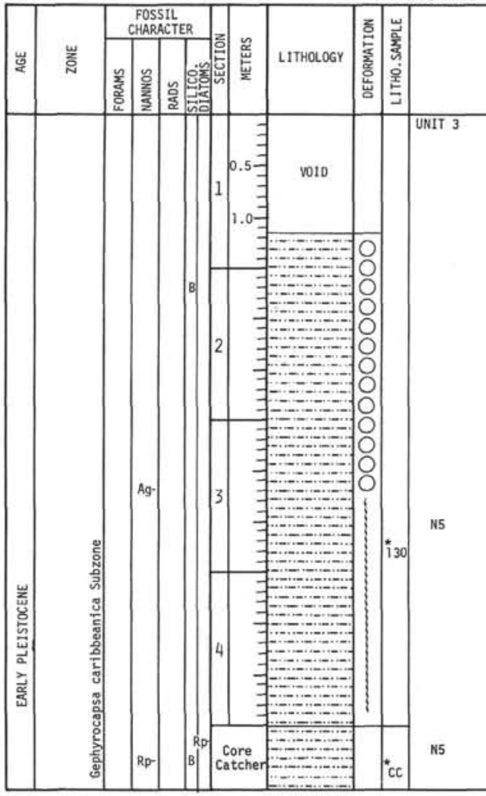

LITHOLOGIC DESCRIPTION

Color medium gray (N5); drilling breccia to intense deformation.

CLAYEY SILT
Smears: 3-130, CC

Texture	Composition
50% Silt	79-87% Clay minerals
30-45% Clay	10% Feldspar
5-20% Sand	2% Heavy minerals
	2% Volcanic glass
	Tr- 5% Nannofossils
	1% Diatoms
	1% Radiolarians
	1% Sponge spicules

Carbon Carbonate 3-130
0.7, 0.4, 2

Explanatory notes in chapter 1

Site 297 Hole Core 8 Cored Interval: 105.5-115.0 m

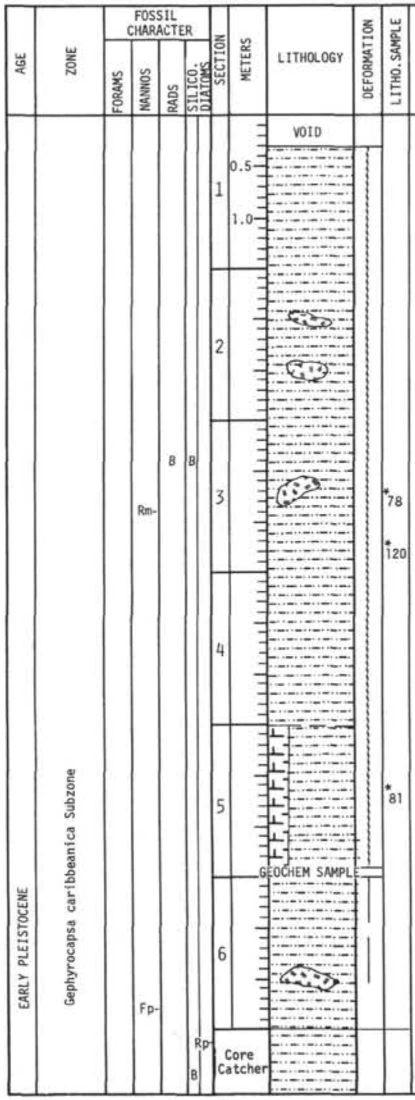

LITHOLOGIC DESCRIPTION

Generally medium gray (N5-N6) intense drilling deformation at top - moderate at base.

CLAYEY SILT
Smear: 3-120

Texture	Composition
50% Silt	80% Clay minerals
40% Clay	7% Quartz
10% Sand	3% Feldspar
	3% Heavy minerals
	3% Volcanic glass
	2% Micarb
	1% Zeolite
	Tr% Foraminifera
	Tr% Nannofossils
	Tr% Sponge spicules
	Tr% Radiolarians

NANNOFOSSIL-RICH CLAYEY SILT
Smear: 5-81

Texture	Composition
62% Clay	74% Clay minerals
38% Silt	12% Nannofossils
	4% Heavy minerals
	4% Feldspar
	3% Quartz
	3% Volcanic glass
	2% Micarb
	1% Zeolite
	Tr% Foraminifera
	Tr% Radiolarians
	Tr% Sponge spicules

N5-N6

VOLCANIC ASH
Smear: 3-78

Texture	Composition
65% Sand	91% Volcanic glass
25% Silt	5% Feldspar
10% Clay	3% Heavy minerals
	1% Quartz

Up to 25% opaques in 3-83.

Grain Size 5-80
0.1, 38.0, 61.9

Carbon Carbonate 5-78
0.8, 0.4, 3

N5-N6

Explanatory notes in chapter 1

Site 297 Hole Core 9 Cored Interval: 124.5-134.0 m

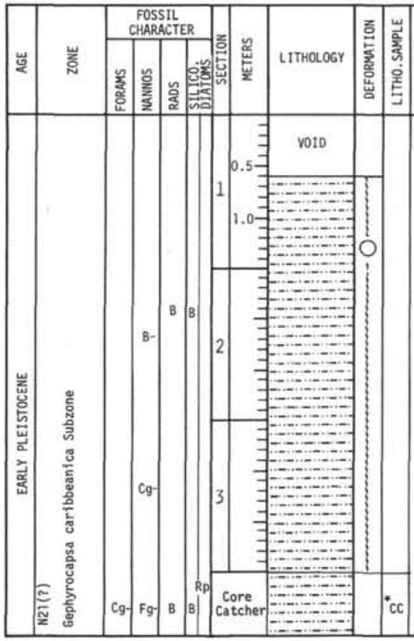

LITHOLOGIC DESCRIPTION

Color dark green gray (5GY 4/1); intense drilling deformation, some stiff zones.

SILTY CLAY
Smear: CC

Texture	Composition
55% Clay	88% Clay minerals
40% Silt	3% Quartz
5% Sand	2% Feldspar
	2% Volcanic glass
	2% Micarb
	1% Zeolite
	1% Heavy minerals
	Tr% Radiolarians
	Tr% Sponge spicules

5GY 4/1

5GY 4/1

Explanatory notes in chapter 1

Site 297 Hole Core 10 Cored Interval: 153.0-162.5

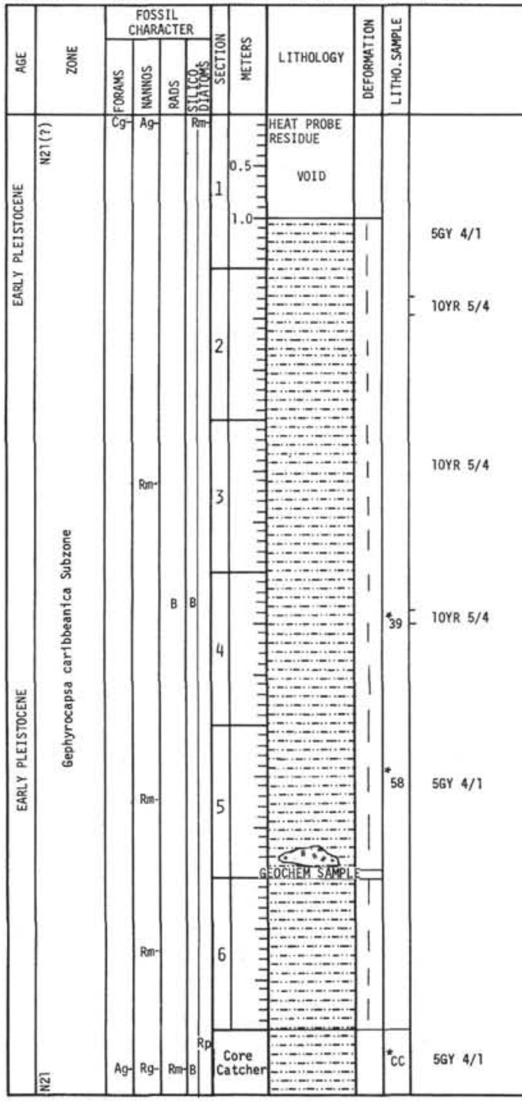

LITHOLOGIC DESCRIPTION

Slight drilling deformation; dark greenish gray (5GY 4/1) with few dusky yellow green areas (10GY 3/2); some pyritized burrows - streaking of green, purple colors in Section 6; some lithification in Section 6.

SILTY CLAY

Smears: 4-39, 5-58, CC

Texture	Composition
55-60% Clay	75-77% Clay minerals
40-45% Silt	7-10% Quartz
	5- 7% Volcanic glass
	3% Feldspar
	3% Zeolite
	2% Heavy minerals
	0- 3% Glauconite
	Tr% Sponge spicules

Explanatory notes in chapter 1

Site 297 Hole Core 11 Cored Interval: 200.5-210.0 m

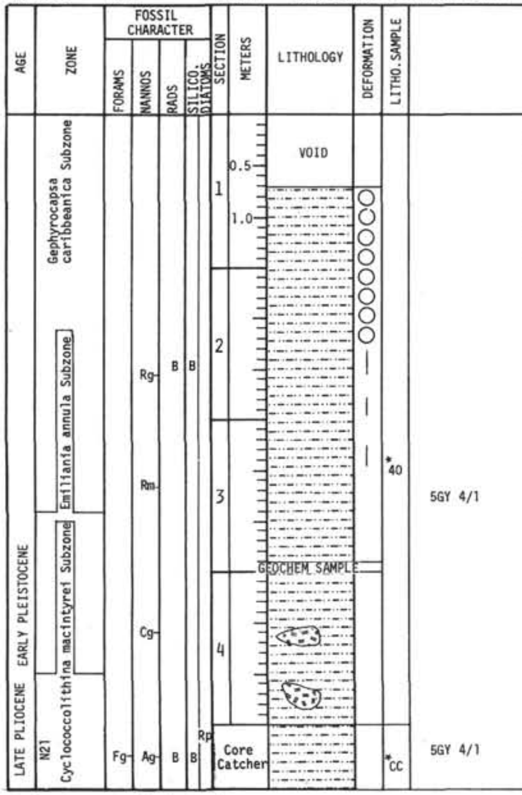

LITHOLOGIC DESCRIPTION

Dark greenish gray (5GY 4/1); intense drilling deformation; lithification throughout sections.

SILTY CLAY

Smears: 3-40, CC

Texture	Composition
60% Clay	85% Clay minerals
40% Silt	3-15% Quartz
	4- 5% Volcanic glass
	2- 3% Feldspar
	2- 3% Zeolite
	2% Heavy minerals
	0- 2% Micronodules
	1% Micarb
	1% Sponge spicules

Explanatory notes in chapter 1

Site 297 Hole Core 12 Cored Interval: 248.0-257.5 m

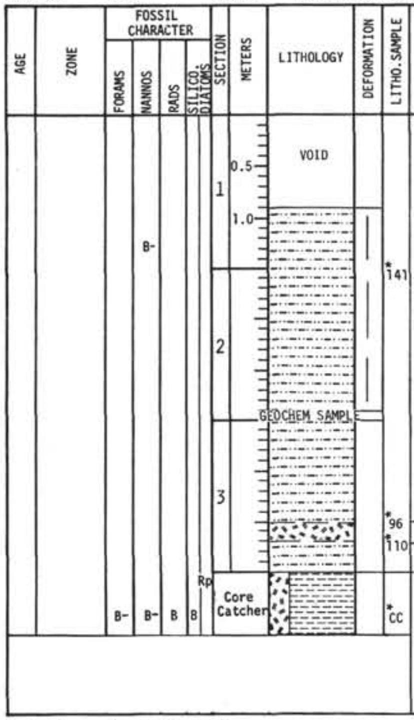

LITHOLOGIC DESCRIPTION

Color olive gray (5Y 4/1) semilithified; moderate drilling deformation; faint laminations - sandy clay zones; bioturbated.

SILTY CLAYSTONE
Smears: 1-141, 3-96

Texture	Composition
58% Clay	80-89% Clay minerals
42% Silt	4- 6% Feldspar
	3- 4% Volcanic glass
	2- 7% Mica
	1- 3% Heavy minerals
	1% Micarb

5Y 5/1

VOLCANIC ASH
Smear: 3-110

Composition
97% Volcanic glass
2% Quartz
3% Feldspar

ASH-RICH SILTY CLAY
Smear: CC

Texture	Composition
70% Clay	81% Clay minerals
30% Silt	11% Volcanic glass
	7% Feldspar
	2% Heavy minerals

5YR 6/1 -
5G 4/1

Grain Size 2-68
0.4, 41.7, 57.8

X-ray 2-66 (Bulk)
36.6% Quar
32.9% Mica
19.6% Plag
5.5% Chlo
5.4% Mont

Explanatory notes in chapter 1

Site 297 Hole Core 13 Cored Interval: 295.5-305.0 m

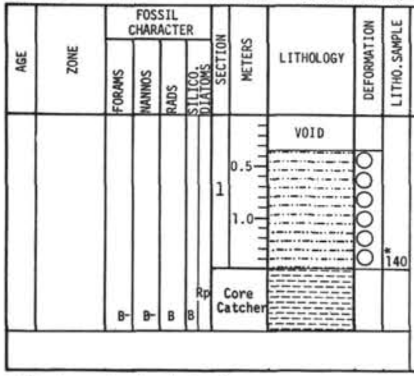

LITHOLOGIC DESCRIPTION

Olive gray (5Y 4/1); brecciated, indurated, bioturbation; some ash zones.

5Y 4/1

SILTY CLAYSTONE
Smear: 1-140

Texture	Composition
61% Clay	84% Clay (Sericite)
39% Silt	15% Mica
	1% Feldspar
	Tr% Quartz

Grain Size 1-140
0.1, 38.7, 61.2

Explanatory notes in chapter 1

Site 297 Hole Core 14 Cored Interval: 314.5-324.0 m

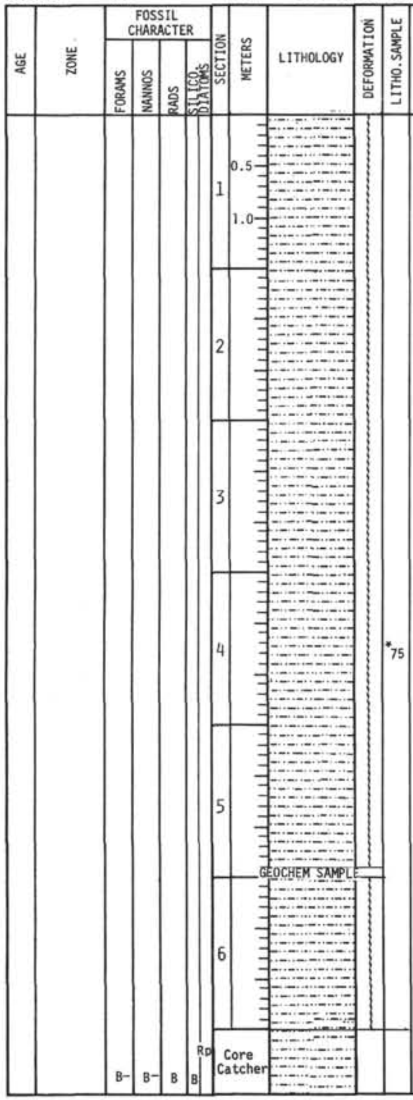

LITHOLOGIC DESCRIPTION

Color olive gray (5Y 4/1); intense drilling deformation and brecciation; slight to moderate mottling.

SILTY CLAYSTONE
Smear: 4-75

Texture	Composition
68% Clay	90% Clay minerals
32% Silt	4% Feldspar
	3% Mica
	2% Heavy minerals
	1% Micarb
	Tr% Nannofossils

Grain Size 4-74
0.1, 31.6, 68.3

X-ray 4-72 (Bulk)
34.0% Mica
33.4% Quar
15.6% Plag
12.1% Mont
4.9% Chlo

5Y 4/1

5Y 4/1

5Y 4/1

Explanatory notes in chapter 1

Site 297 Hole Core 15 Cored Interval: 333.5-343.0 m

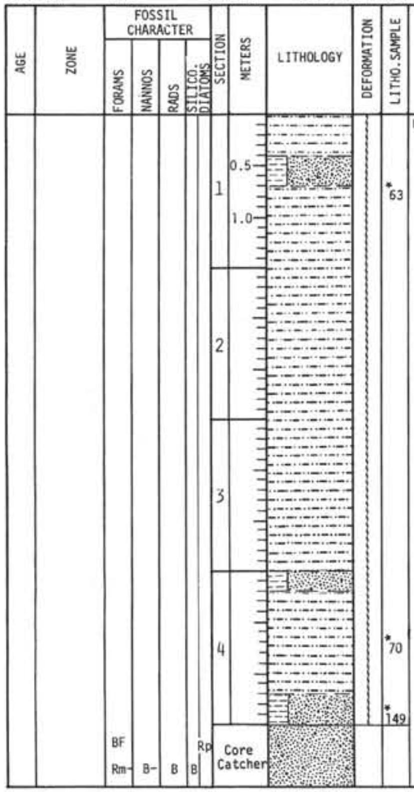

LITHOLOGIC DESCRIPTION

UNIT 4

5Y 5/1

5GY 4/1

Olive gray (5Y 5/1); intense drilling deformation; color mottling, vertical streaking of silts-sands.

SILTY CLAYSTONE
Smear: 4-70

Texture	Composition
71% Clay	80% Clay minerals
29% Silt	10% Mica
	5% Feldspar
	5% Quartz

CLAY-RICH SILTY SAND
Smears: 1-63, 4-149

Texture	Composition
40-50% Sand	45% Mudstone clasts
30% Silt	20-58% Quartz
20-30% Clay	20-30% Clay minerals
	10-15% Feldspar
	2% Heavy minerals
	0-10% Volcanic glass
	Tr% Pyrite
	Tr% Foraminifera

Grain Size 4-70
02., 28.6, 71.2

Explanatory notes in chapter 1

Site 297 Hole Core 16 Cored Interval: 352.5-362.0 m

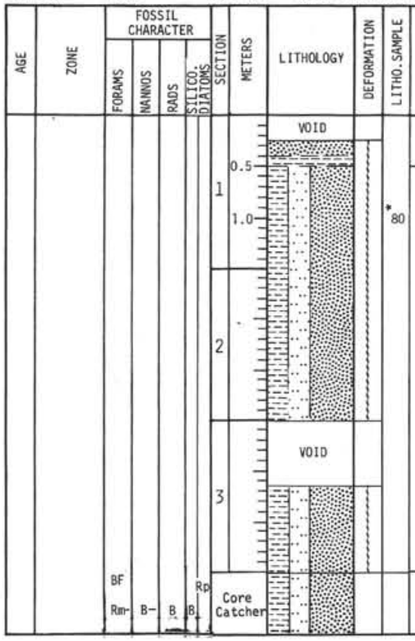

LITHOLOGIC DESCRIPTION

5Y 4/1

5Y 2/1

5GY 4/1

Colors olive gray (5Y 4/1), olive black (5Y 2/1); intense drilling deformation; peat and wood noted in Section 2.

CLAY/SILT-RICH SAND
Smear: 1-80

Texture	Composition
60% Sand	40% Quartz
20% Silt	29% Opaques
20% Clay	20% Clay minerals
	10% Feldspar
	1% Heavy minerals

Site 297 Hole Core 17 Cored Interval: 395.5-400.0 m

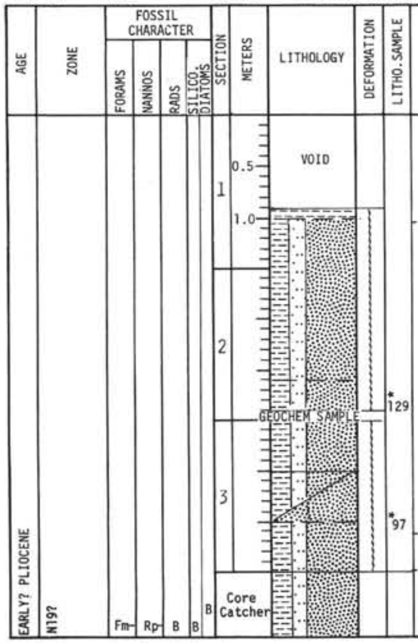

LITHOLOGIC DESCRIPTION

5Y 4/1

5Y 2/1

5Y 4/1

5Y 2/1

5GY 4/1

Colors olive gray (5Y 4/1), olive black (5Y 2/1); intense drilling deformation; peat in Section 2.

CLAY/SILT-RICH SAND

CLAYSTONE
Smear: 3-97

Texture	Composition
95% Clay	94% Clay minerals
5% Silt	3% Feldspar
	1% Volcanic glass
	2% Plant Debris

PEAT-RICH-ASHY SILT
Smear: 2-129

Texture	Composition
60% Silt	30% Clay minerals
30% Clay	30% Volcanic glass
10% Sand	15% Organic
	10% Quartz
	10% Feldspar
	3% Heavy minerals
	1% Mica
	1% Glauconite

Explanatory notes in chapter 1

Site 297 Hole Core 18 Cored Interval: 428.5-438.0 m

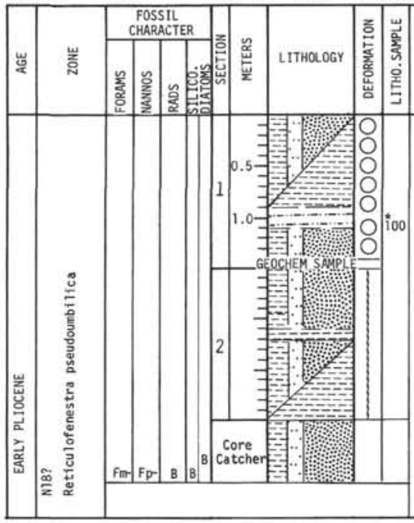

LITHOLOGIC DESCRIPTION

Color olive gray (5Y 4/1) - drilling breccia.

CLAYSTONE: SILT/CLAY-RICH SAND

CLAYEY SILT
Smear: 1-100

Texture	Composition
69% Silt	45% Quartz
21% Clay	28% Lithic fragments
10% Sand	25% Feldspar
	2% Heavy minerals
	Tr% Mica

5Y 4/1

Biotite and zircon.

Grain Size 2-84
10.2, 68.8, 21.0

5GY 4/1

Explanatory notes in chapter 1

Site 297 Hole Core 19 Cored Interval: 466.5-476.0 m

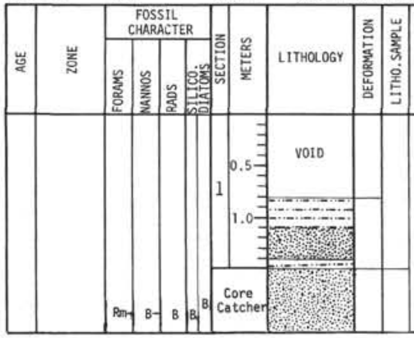

LITHOLOGIC DESCRIPTION

Color medium dark gray (N4) with olive black (5Y 2/1) and olive gray (5Y 4/1); intense drilling deformation; some graded bedding, faint laminations, plant fragments.

N4
5Y 2/1
5Y 4/1

SILTY SAND

CLAYEY SILTSTONE

Grain Size 1-99
2.0, 56.8, 41.2

Grain Size 1-130
56.2, 28.4, 15.4

5Y 2/1
5Y 4/1

Explanatory notes in chapter 1

Site 297 Hole Core 20 Cored Interval: 504.5-514.0 m

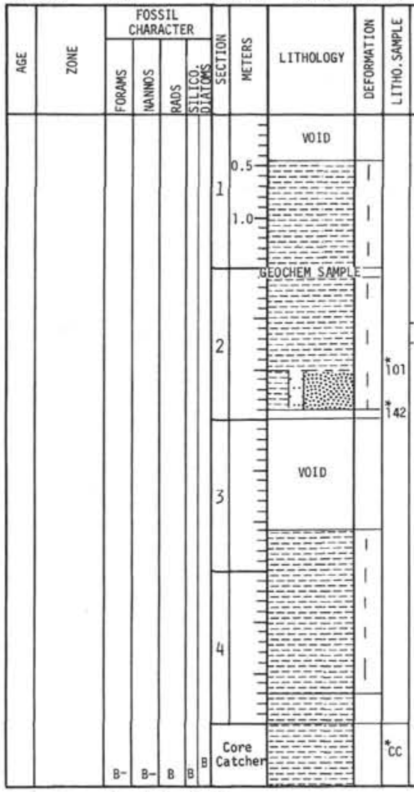

LITHOLOGIC DESCRIPTION

Colors dark greenish gray (5GY 4/1) to medium dark gray (N4); pre-turbidite clay; stiff-chunky with slight drilling deformation; some graded beds; chondrites.

5GY 4/1 with N4

CLAYSTONE
Smears: 2-101, CC

Texture	Composition
95% Clay	94% Clay minerals
5% Silt	3% Heavy minerals, opaques
	1% Quartz
	1% Volcanic glass
	1% Zeolite

5GY 4/1

10GY 4/2

SILT/SAND-RICH CLAY
Smear: 2-142

Texture	Composition
65% Clay	56% Clay minerals
20% Silt	30% Quartz
15% Sand	10% Feldspar
	3% Heavy minerals
	1% Mica
	Tr% Clauconite

5Y 2/1
N7

5Y 2/1
5GY 2/1

5Y 2/1 -
5GY 4/1

5GY 4/1

Explanatory notes in chapter 1

Site 297 Hole Core 21 Cored Interval: 523.5-533.0 m

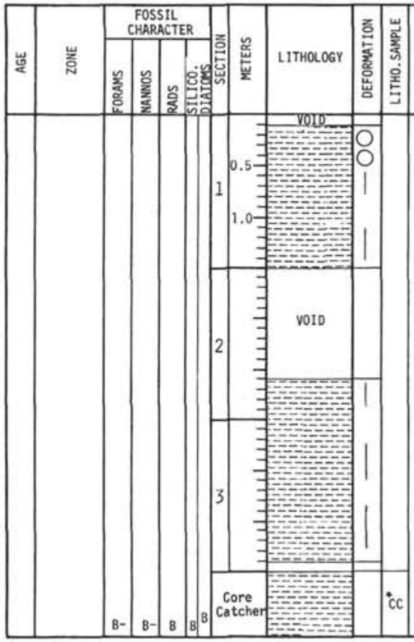

LITHOLOGIC DESCRIPTION

Color dark greenish gray (5GY 4/1); thin + medium irregular bedding with color variations; slight drilling deformation - stiff; few chondrites.

CLAYSTONE
Smear: CC

Texture	Composition
93% Clay	92% Clay minerals
7% Silt	3% Quartz
	3% Heavy minerals, opaques
	1% Feldspar
	1% Zeolite
	Tr% Nannofossils

5GY 4/1

5GY 4/1

Explanatory notes in chapter 1

Site 297 Hole Core 22 Cored Interval: 552.0-561.5 m

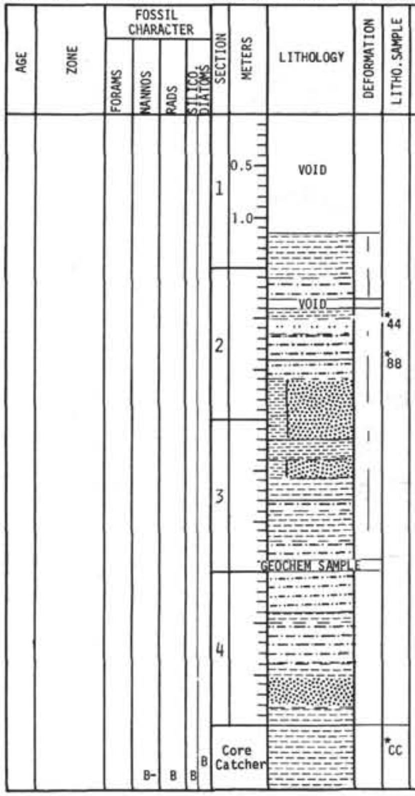

LITHOLOGIC DESCRIPTION

Color dark greenish gray (5GY 4/1), stiff, soft, laminae distinct-to-indistinct, varying thickness slight-moderate deformation; grading in turbidite sequence; plant fragments; some foreset bedding.

Sequence
(Section 2; Section 3)

d
c
b
e
d
c
b
e
d
c
b

CLAYSTONE
Smears: 2-44, CC

Texture	Composition
95% Clay	95% Clay minerals
5% Silt	3% Quartz
	1% Heavy minerals
	1% Volcanic glass

SAND-SILT-CLAY
Smears: 2-88

Texture	Composition
46% Silt	58% Clay minerals
29% Sand	30% Quartz
25% Clay	5% Feldspar
	3% Heavy minerals
	2% Glauconite
	1% Mica
	1% Micarb
	Tr% Foraminifera

5GY 4/1

Grain Size 2-80	Grain Size 3-50
28.9, 46.4, 24.7	0.3, 76.1, 23.7

Grain Size 4-33
3.1, 73.5, 23.4

5GY 4/1

Explanatory notes in chapter 1

Site 297 Hole Core 23 Cored Interval: 590.0-599.5 m

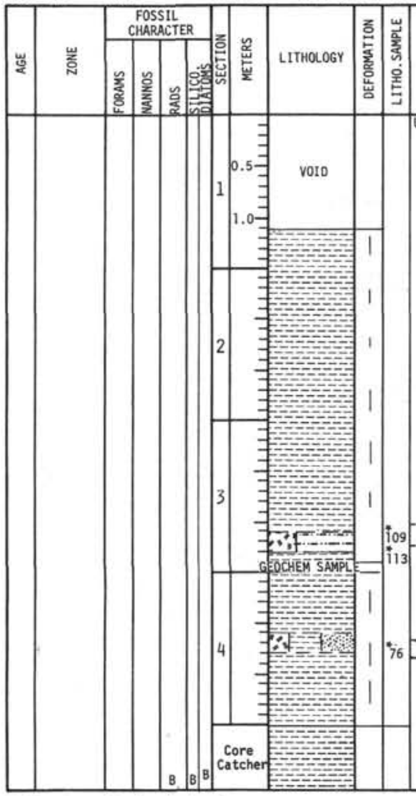

LITHOLOGIC DESCRIPTION

UNIT 5

Color dominately dark greenish gray (5GY 4/1); slight drilling deformation; thin laminations noted as well as graded beds.

5GY 4/1

5Y 2/1

5Y 2/1

5GY 4/1

5GY 4/1

CLAYSTONE

ASHY/CLAYEY SILTSTONE
Smear: 3-109

Texture	Composition
60% Silt	36% Clay minerals
40% Clay	27% Volcanic glass
	19% Feldspar
	8% Quartz
	8% Plant debris
	2% Heavy minerals

ASH-RICH SILTY CLAYSTONE
Smear: 3-113

Texture	Composition
70% Clay	70% Clay minerals
30% Silt	12% Volcanic glass
	10% Feldspar
	5% Quartz
	2% Mica
	1% Heavy minerals
	Tr% Pyrite

ASH-RICH CLAYEY SILTY SAND
Smear: 4-76

Texture	Composition
50% Sand	30% Volcanic glass
30% Silt	20% Opaque
20% Clay	20% Clay minerals
	20% Feldspar
	10% Quartz

Explanatory notes in chapter 1

Site 297 Hole Core 24 Cored Interval: 618.5-628.0 m

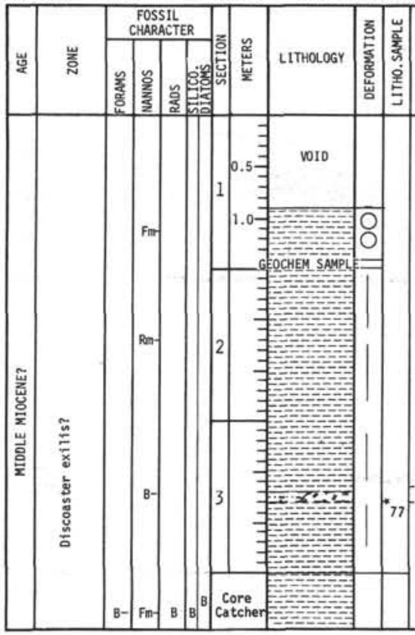

LITHOLOGIC DESCRIPTION

Color dark greenish gray (5GY 4/1) and olive black (5Y 2/1); moderate drilling deformation.

5GY 4/1

5Y 2/1

5GY 4/1

CLAYSTONE

CLAYEY SILTSTONE
(ASHY)
Smear: 3-77

Texture	Composition
53% Silt	46% Clay minerals
47% Clay	25% Volcanic glass
	18% Quartz
	10% Feldspar
	1% Heavy minerals

Grain Size 3-76
0.3, 52.9, 46.7

X-ray 3-76 (Bulk)
37.7% Mont
28.6% Quar
19.2% Mica
12.8% Plag
1.7% Chlo

Explanatory notes in chapter 1

Site 297 Hole Core 25 Cored Interval: 647.0-656.5 m

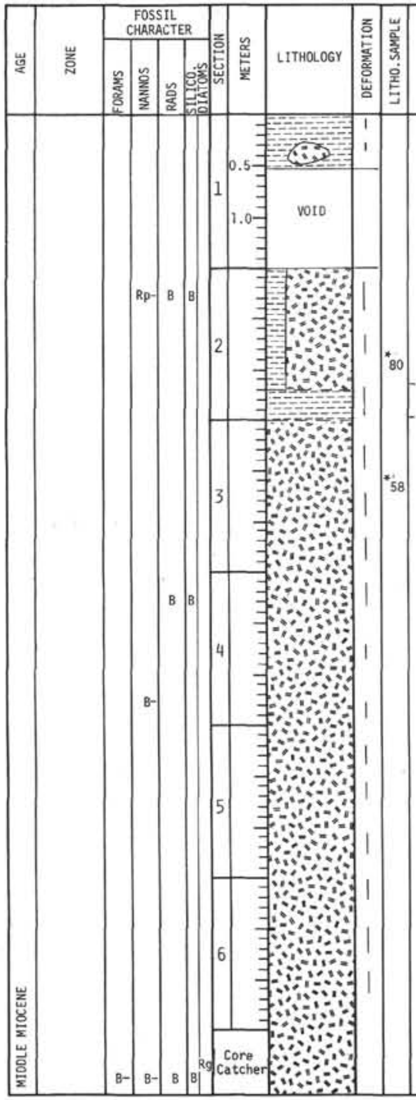

LITHOLOGIC DESCRIPTION

5Y 2/1

Color mainly olive black (5Y 2/1); slight drilling deformation; concretion = ash clay rich pyritic concentration; some slump structures, laminated.

CLAYSTONE

5Y 3/1

PEAT/CLAY-RICH ASH
Smear: 2-80

Texture	Composition
80% Silt	62% Volcanic glass
10% Sand	15% Feldspar
10% Clay	10% Clay minerals
	10% Plant debris
	2% Pyrite
	1% Radiolarians

N4-
5GY 6/1

VOLCANIC ASH
Smear: 3-58

Texture	Composition
85-90% Silt	68-85% Volcanic glass
10% Clay	10-15% Clay minerals
5% Sand	5-25% Feldspar
	1-10% Heavy minerals
	1% Mica
	Tr% Nannofossils

5Y 4/1

5Y 4/1

Explanatory notes in chapter 1

Site 297 Hole Core 26 Cored Interval: 666.0-675.5 m

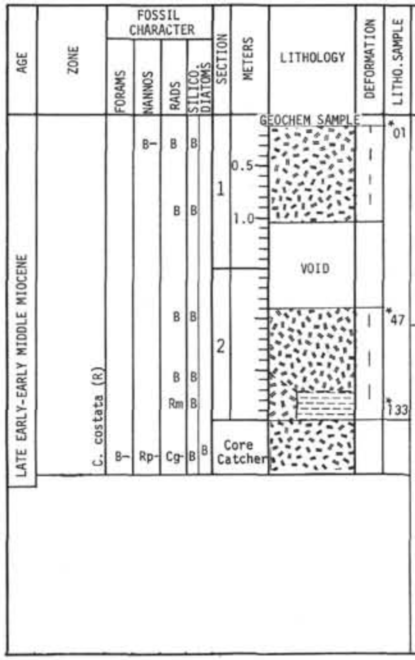

LITHOLOGIC DESCRIPTION

Color dark greenish gray (5GY 4/1) with olive black (5Y 2/1); faint irregular bedding, compact, minor slump structures and grading present.

VOLCANIC (ASH TUFF)
Smears: 1-1, 2-47

Texture	Composition
54% Silt	68-86% Volcanic glass
46% Clay	10% Clay minerals
	2-20% Feldspar
	1- 2% Heavy minerals
	1% Opaques
	Tr% Micarb

N7
5Y 4/1
&
5GY 4/1

ASH-RICH CLAYSTONE
Smear: 2-133

Texture	Composition
90% Clay	60% Clay minerals
10% Silt	18% Quartz
	10% Volcanic glass
	10% Feldspar
	1% Chlorite
	1% Micarb

Grain Size 1-2
0.0, 53.5, 46.5

X-ray 2-133 (Bulk)
34.0% Quar
38.3% Mica
22.8% Mont
13.6% Plag
1.3% Chlo

Explanatory notes in chapter 1

Site 297 Hole Core 27 Cored Interval: 675.5-679.5 m

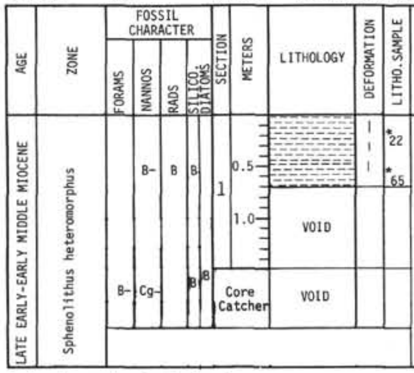

LITHOLOGIC DESCRIPTION

Color medium dark gray (N4); stiff with slight drilling deformation; some green black (5G 2/1) colors.

CLAYSTONE (ASH-BEARING)
Smears: 1-22, 1-65

Texture	Composition
85% Clay	80-85% Clay minerals
15% Silt	10% Mica
	2- 9% Volcanic glass
	2- 6% Feldspar
	1% Heavy minerals

Explanatory notes in chapter 1

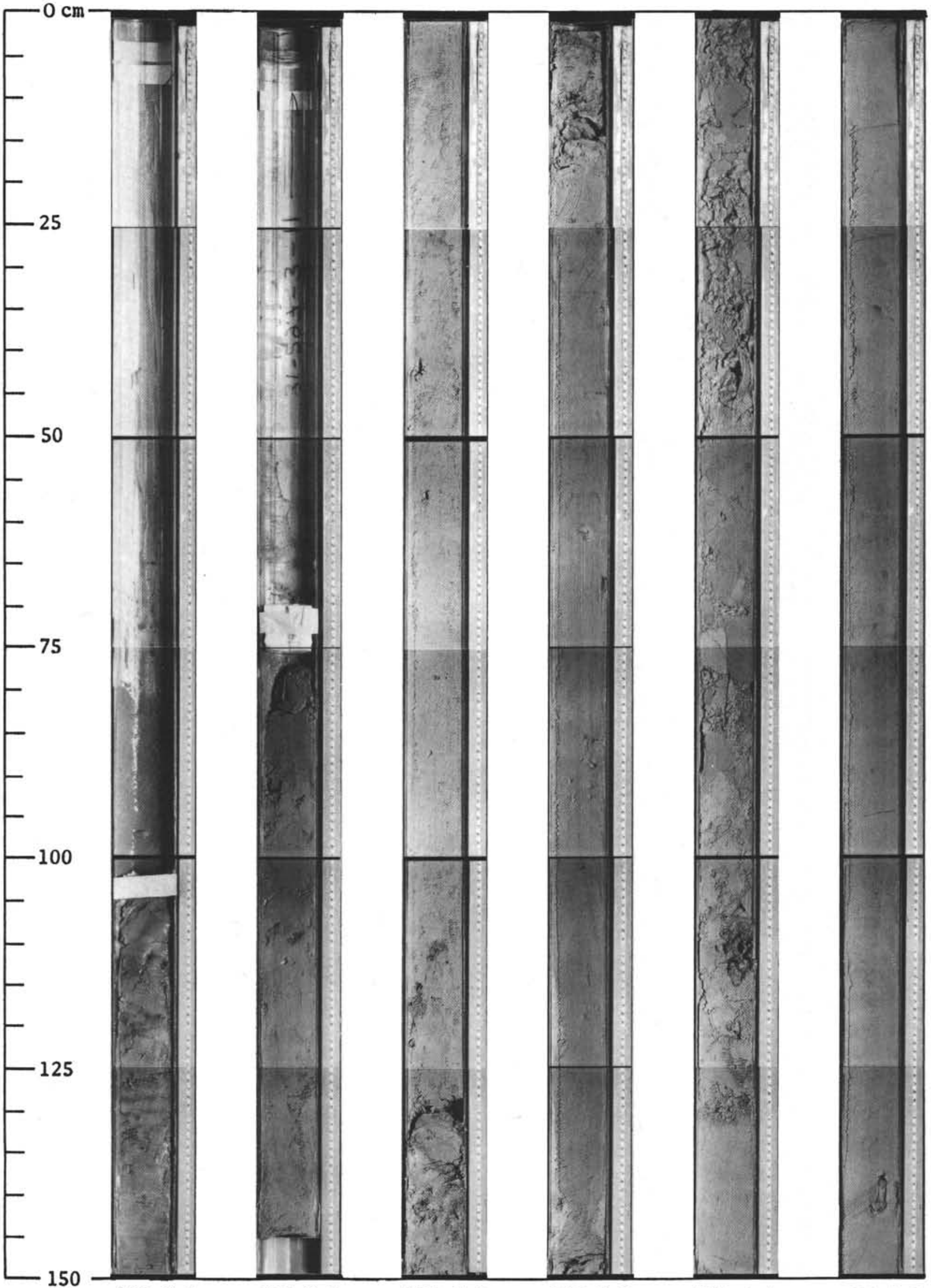
0 cm
25
50
75
100
125
150
297-2-1
297-3-1
297-3-2
297-3-3
297-4-1
297-4-2

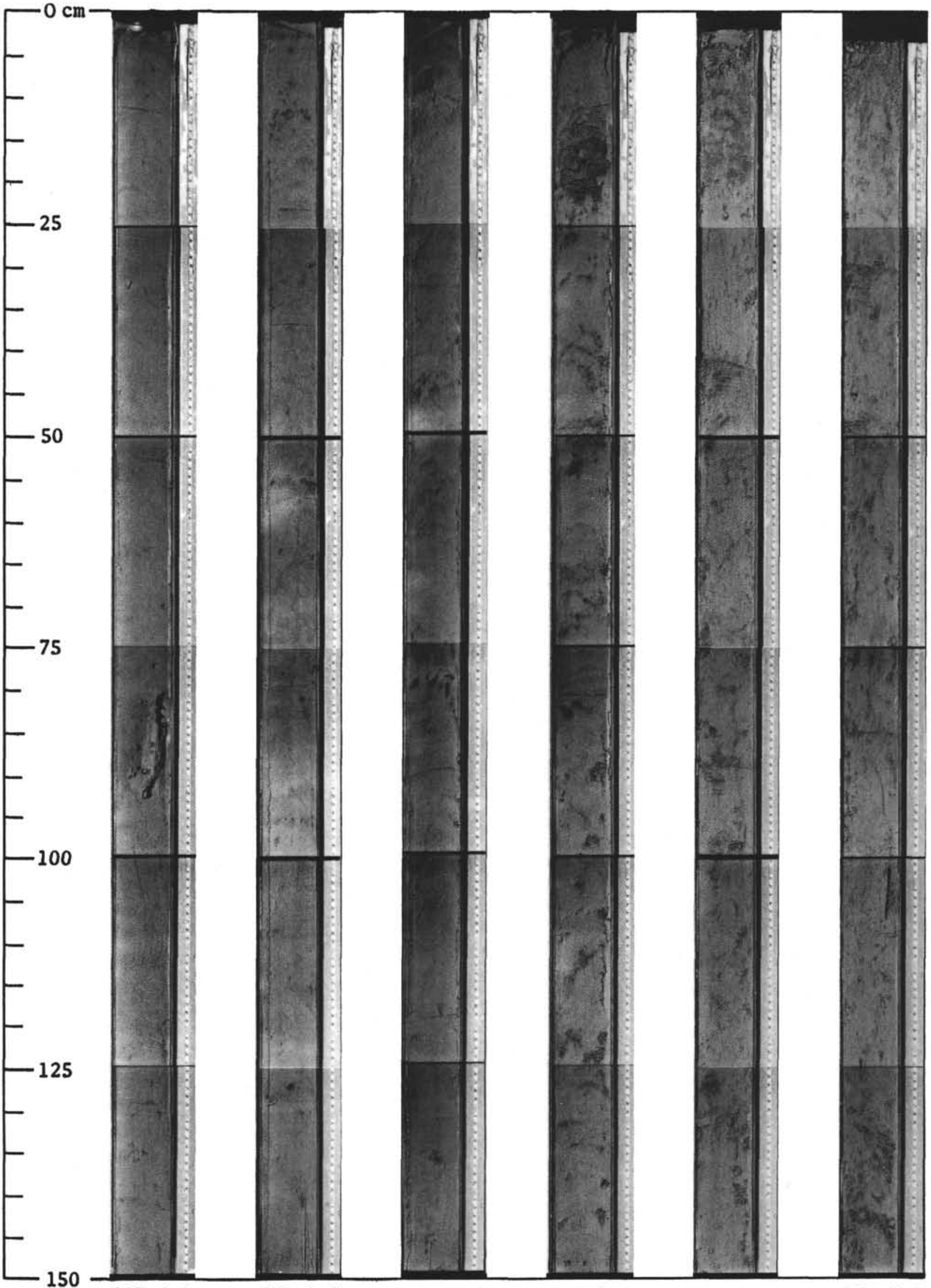
0 cm
25
50
75
100
125
150
297-4-3
297-4-4
297-4-5
297-4-6
297-5-1
297-5-2

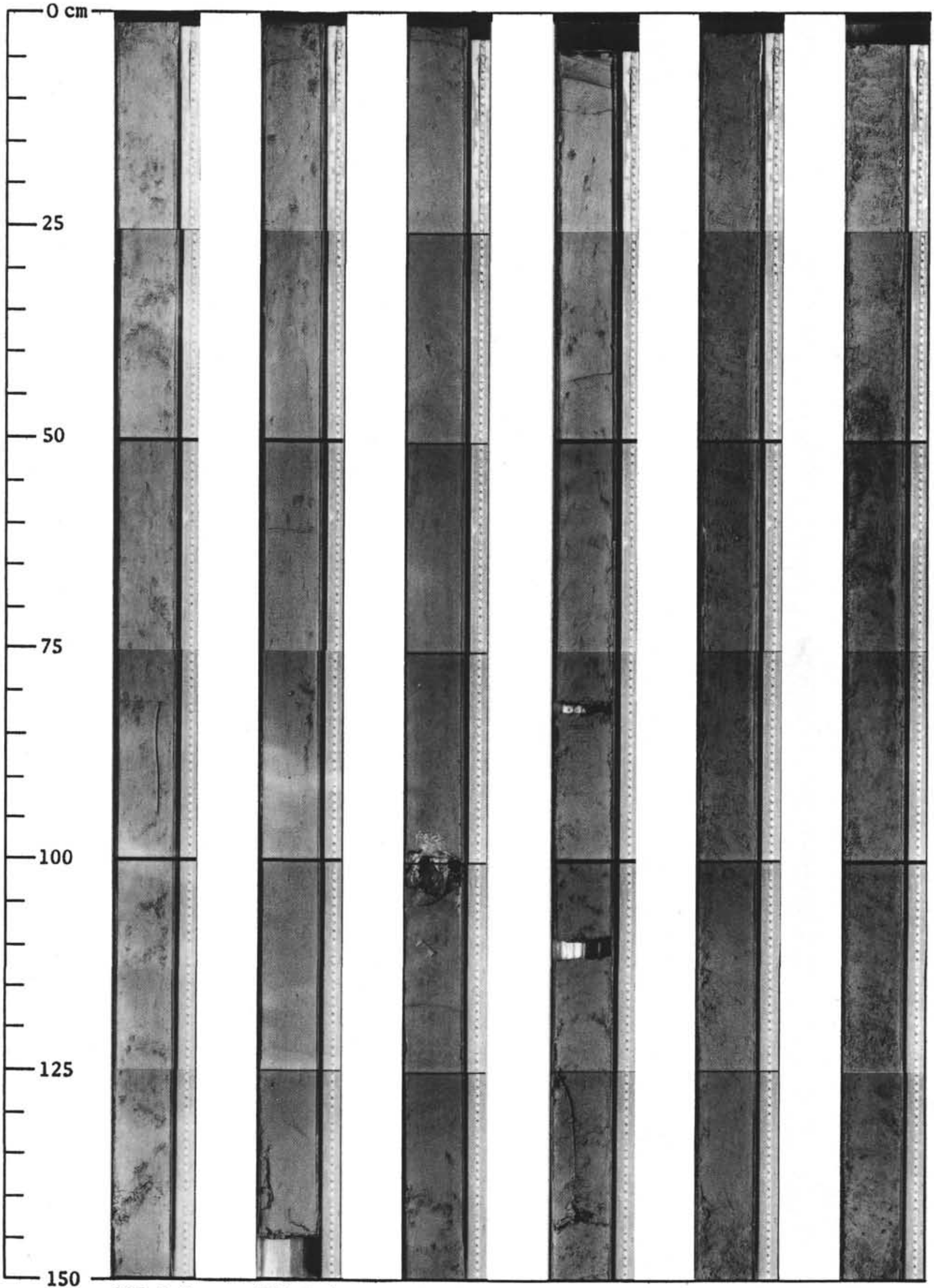
0 cm
25
50
75
100
125
150
297-5-3
297-5-4
297-5-5
297-5-6
297-6-1
297-6-2

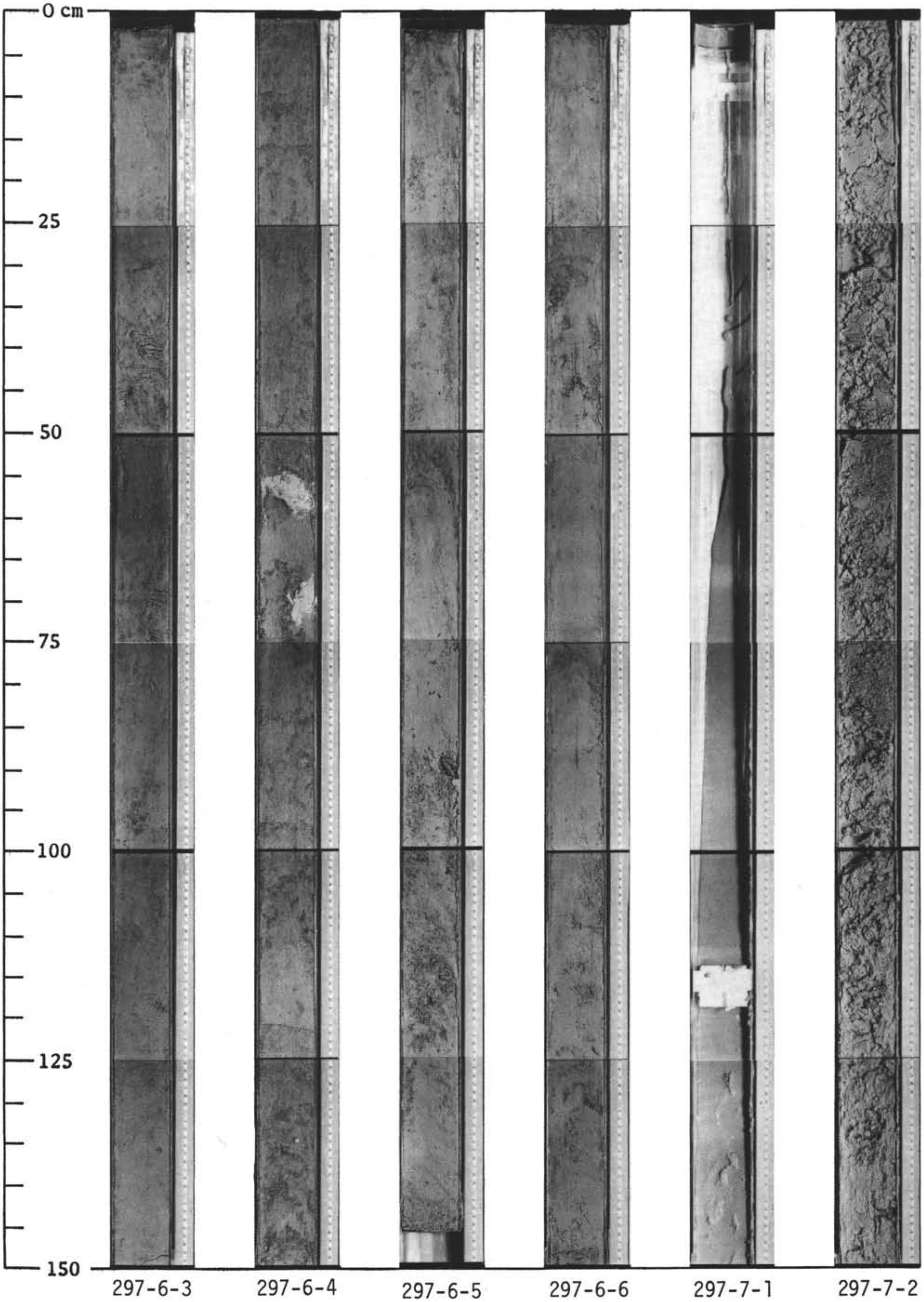
0 cm
25
50
75
100
125
150
297-6-3
297-6-4
297-6-5
297-6-6
297-7-1
297-7-2

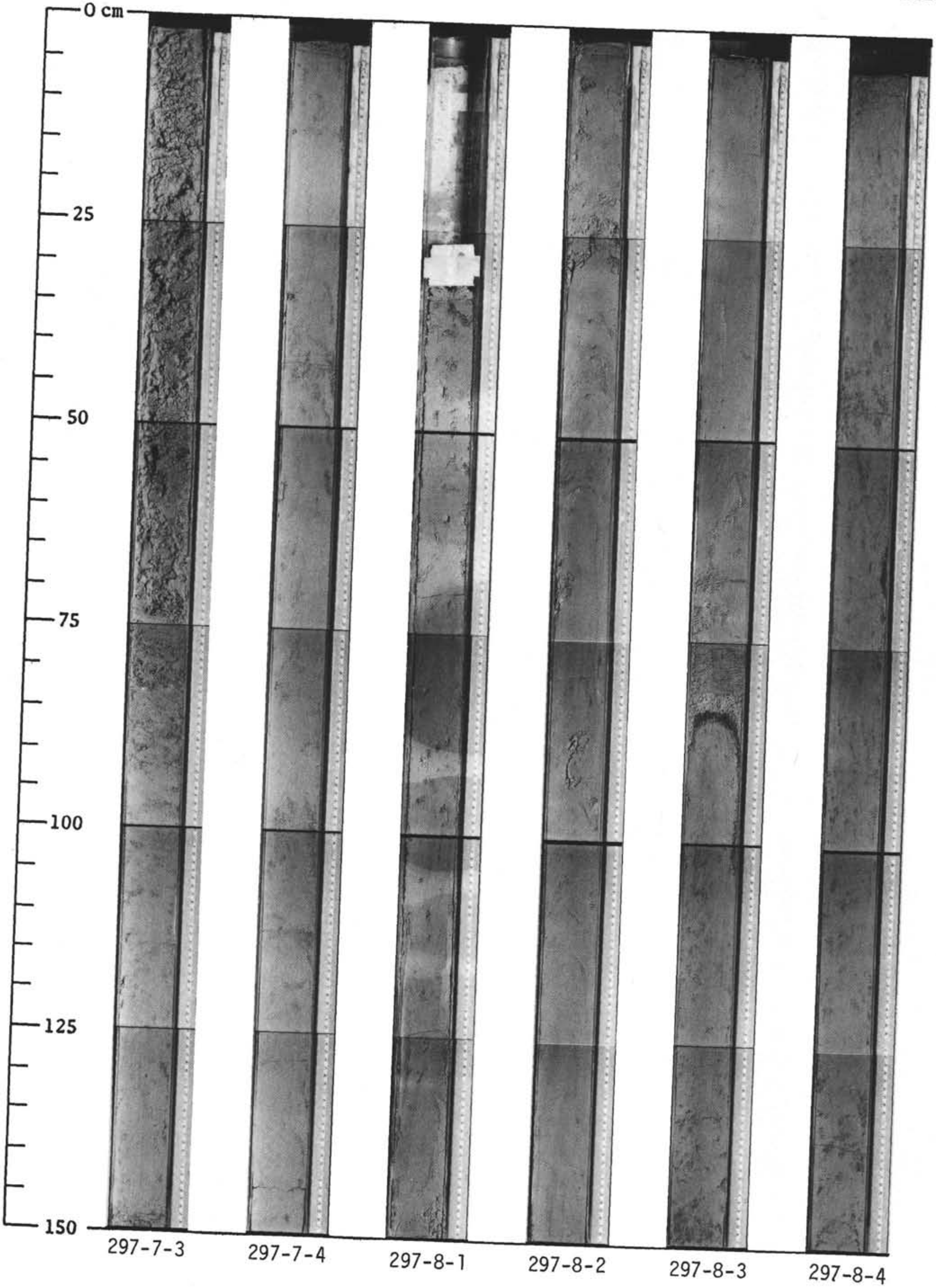
0 cm
25
50
75
100
125
150
297-7-3
297-7-4
297-8-1
297-8-2
297-8-3
297-8-4

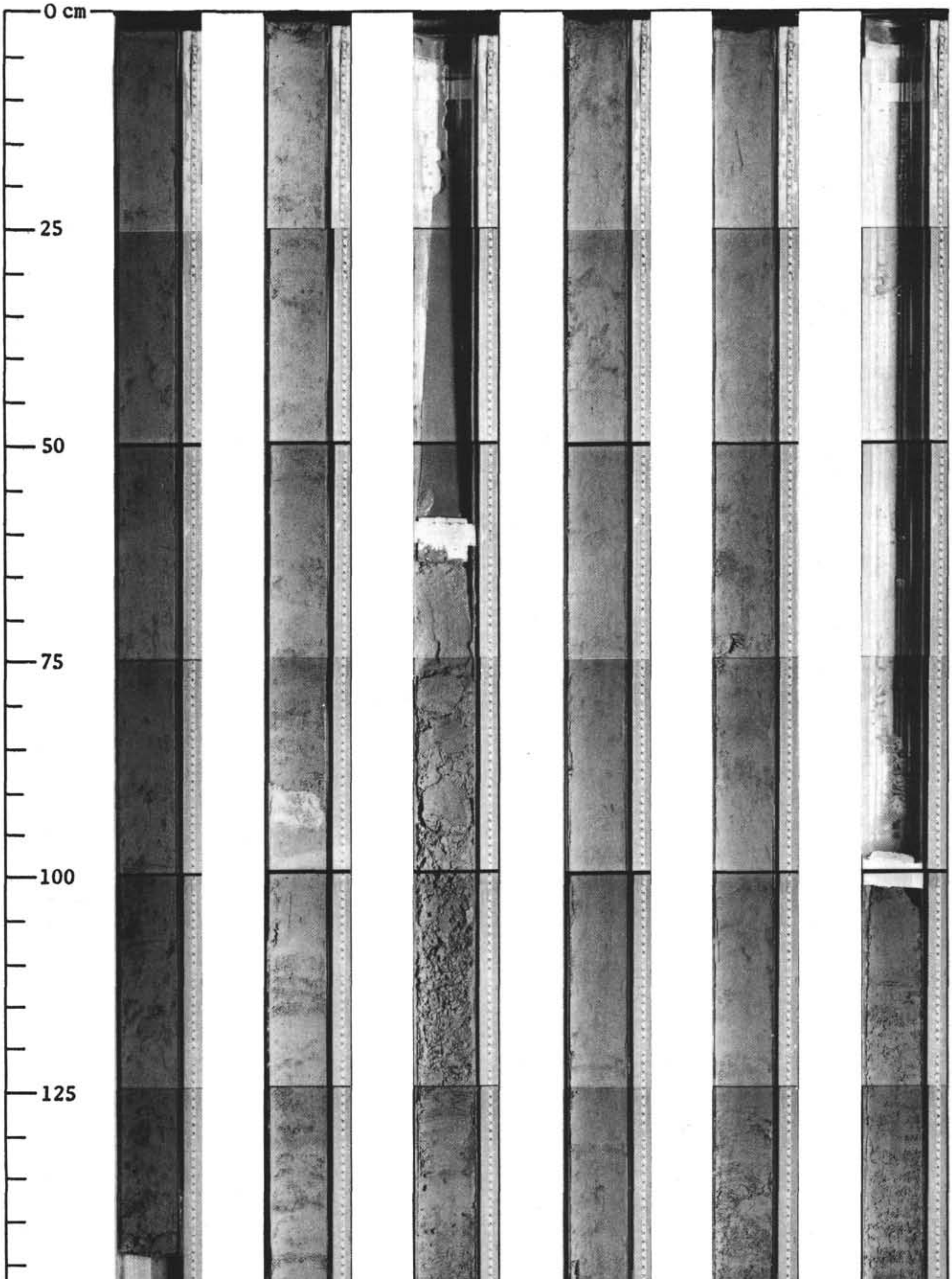
0 cm
25
50
75
100
125
150
297-8-5
297-8-6
297-9-1
297-9-2
297-9-3
297-10-1

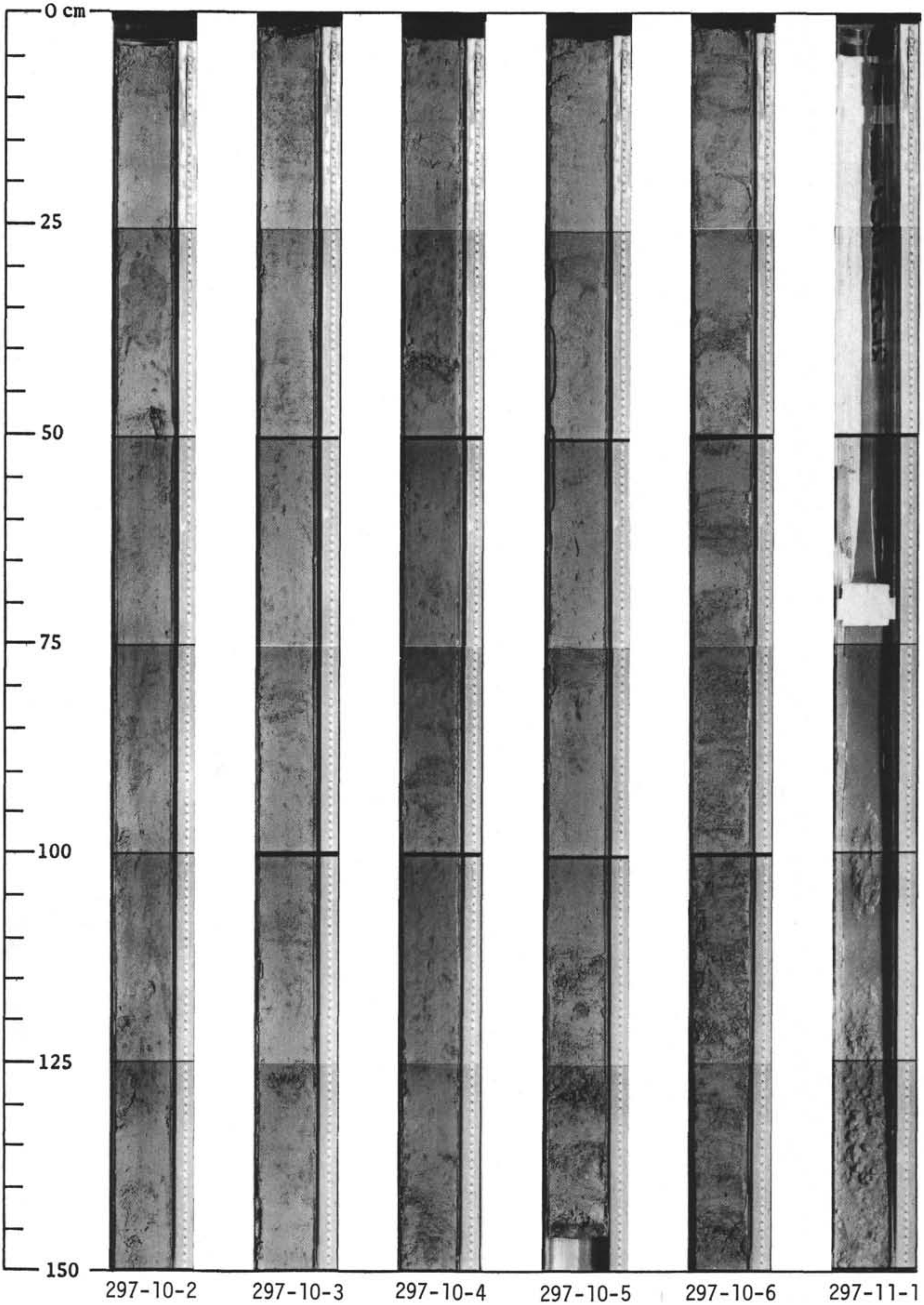
0 cm
25
50
75
100
125
150
297-10-2
297-10-3
297-10-4
297-10-5
297-10-6
297-11-1

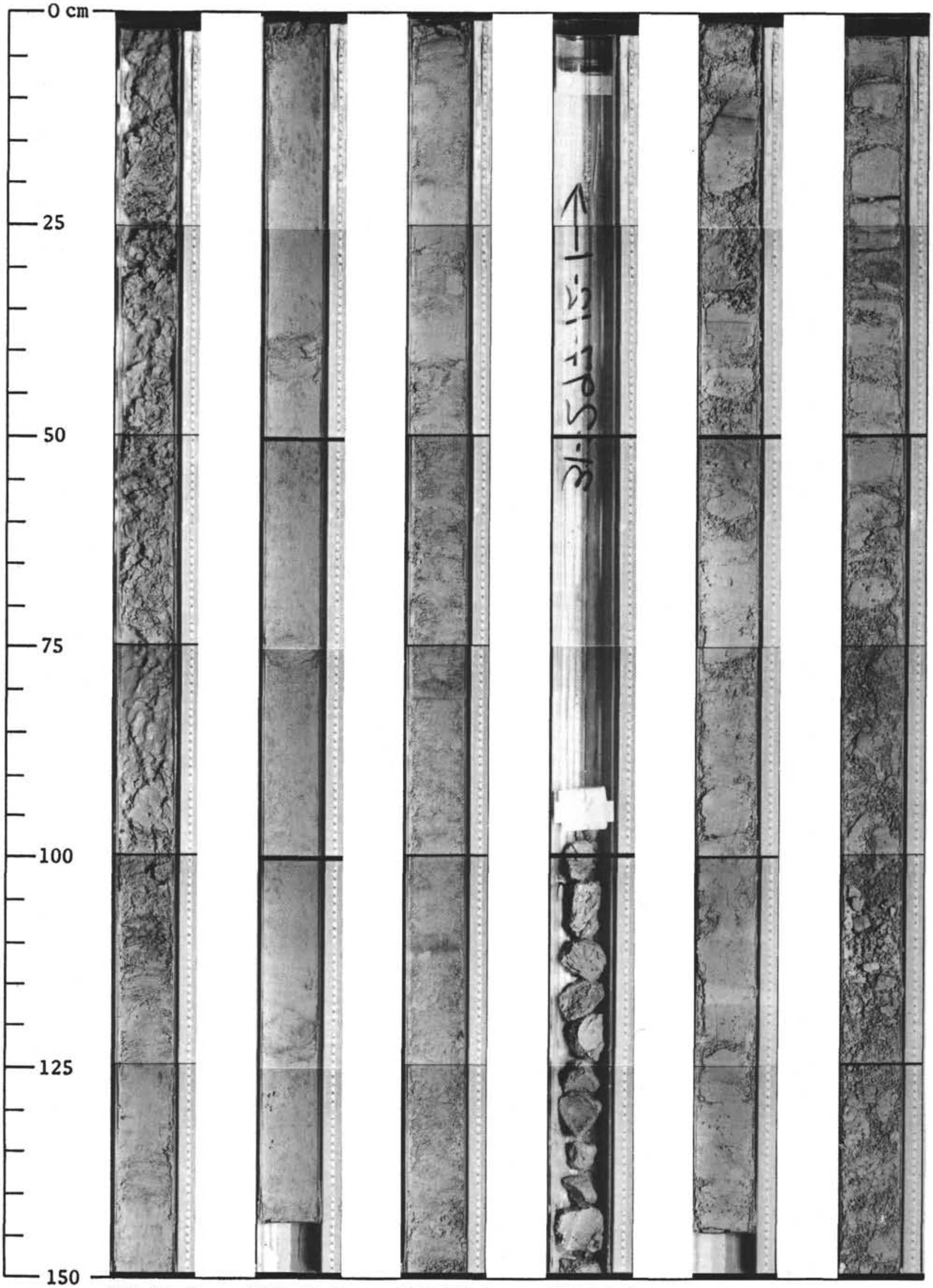
0 cm
25
50
75
100
125
150
297-11-2
297-11-3
297-11-4
297-12-1
297-12-2
297-12-3

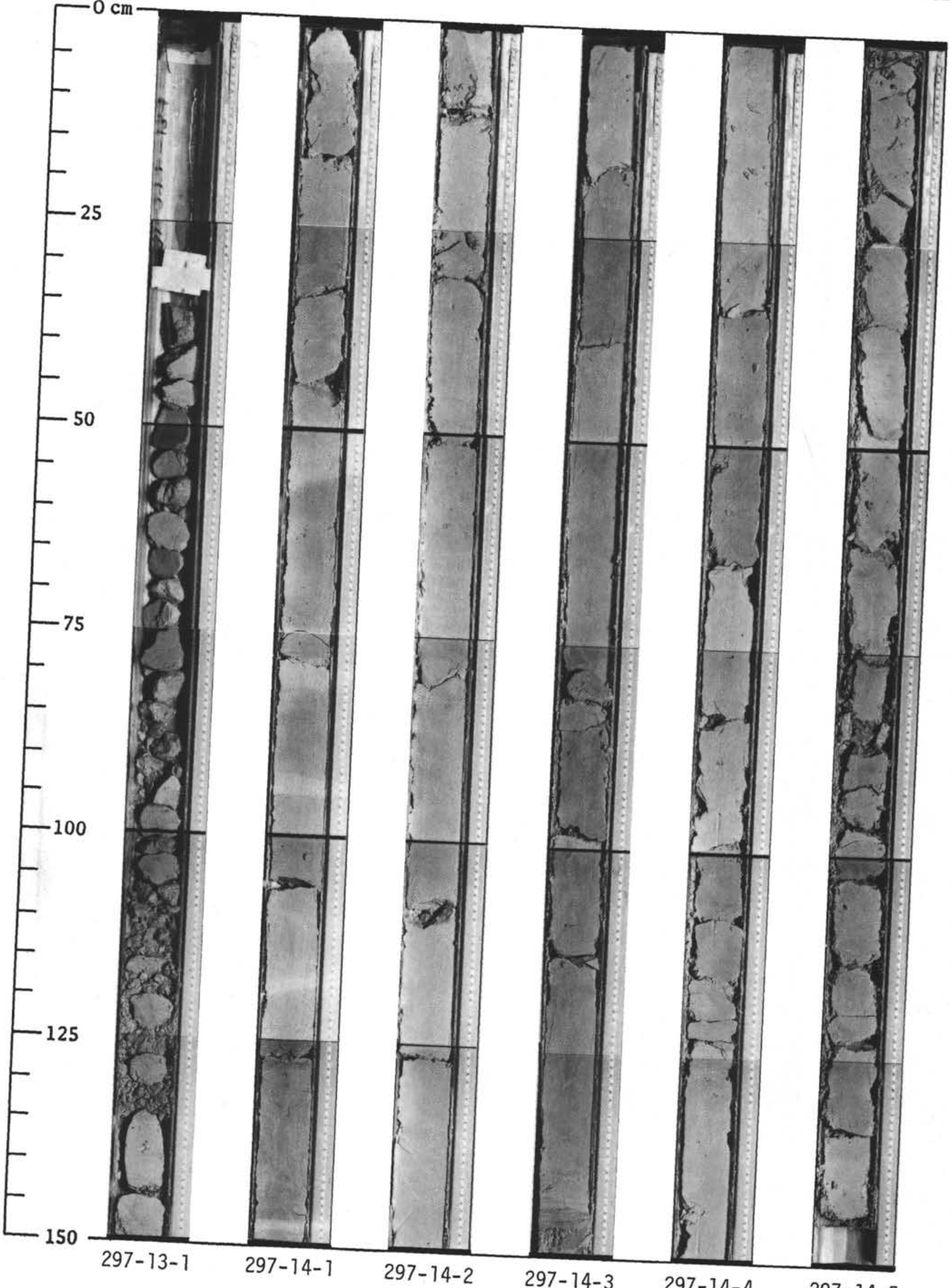
0 cm
25
50
75
100
125
150
297-13-1
297-14-1
297-14-2
297-14-3
297-14-4
297-14-5

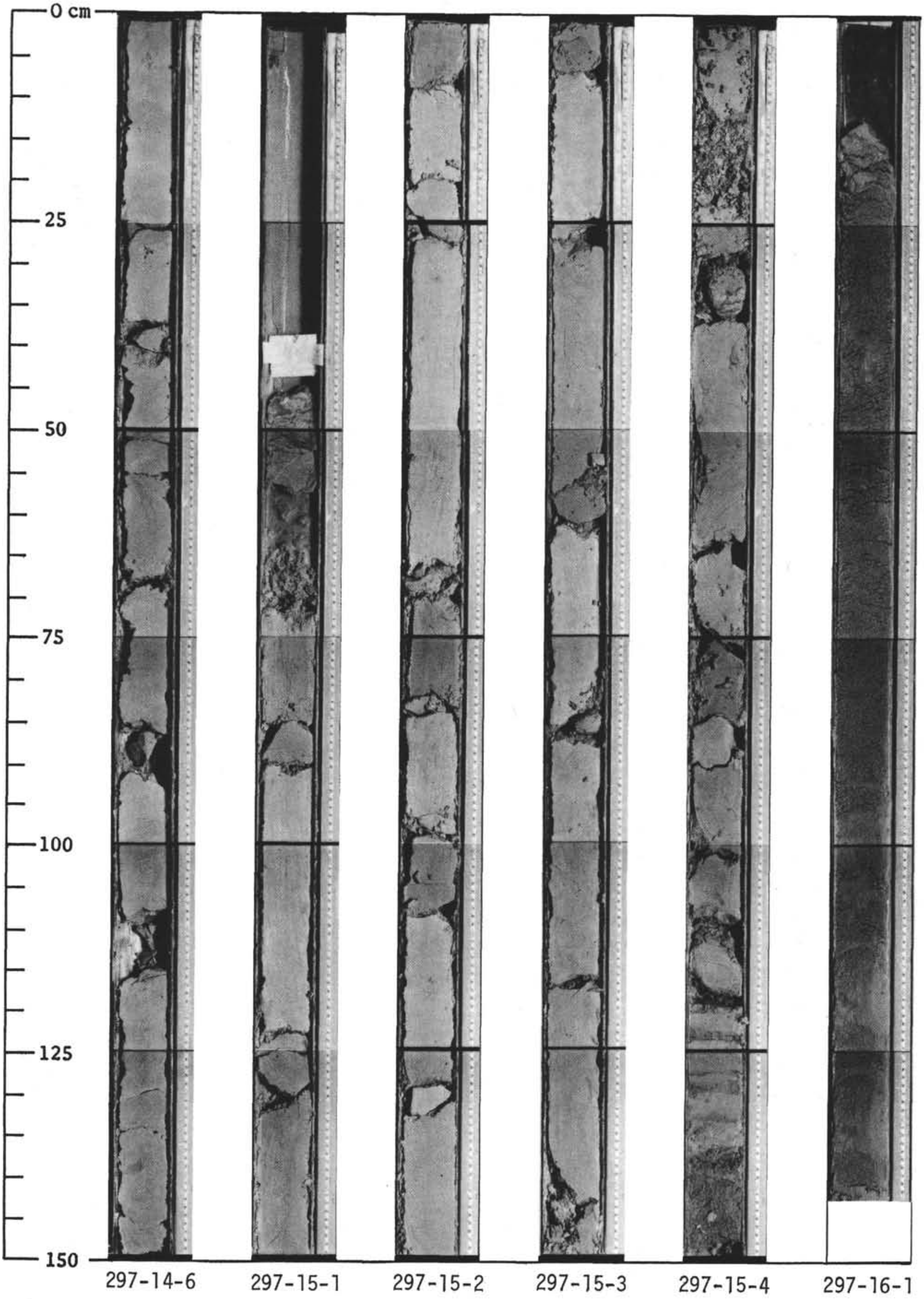
0 cm
25
50
75
100
125
150
297-14-6
297-15-1
297-15-2
297-15-3
297-15-4
297-16-1

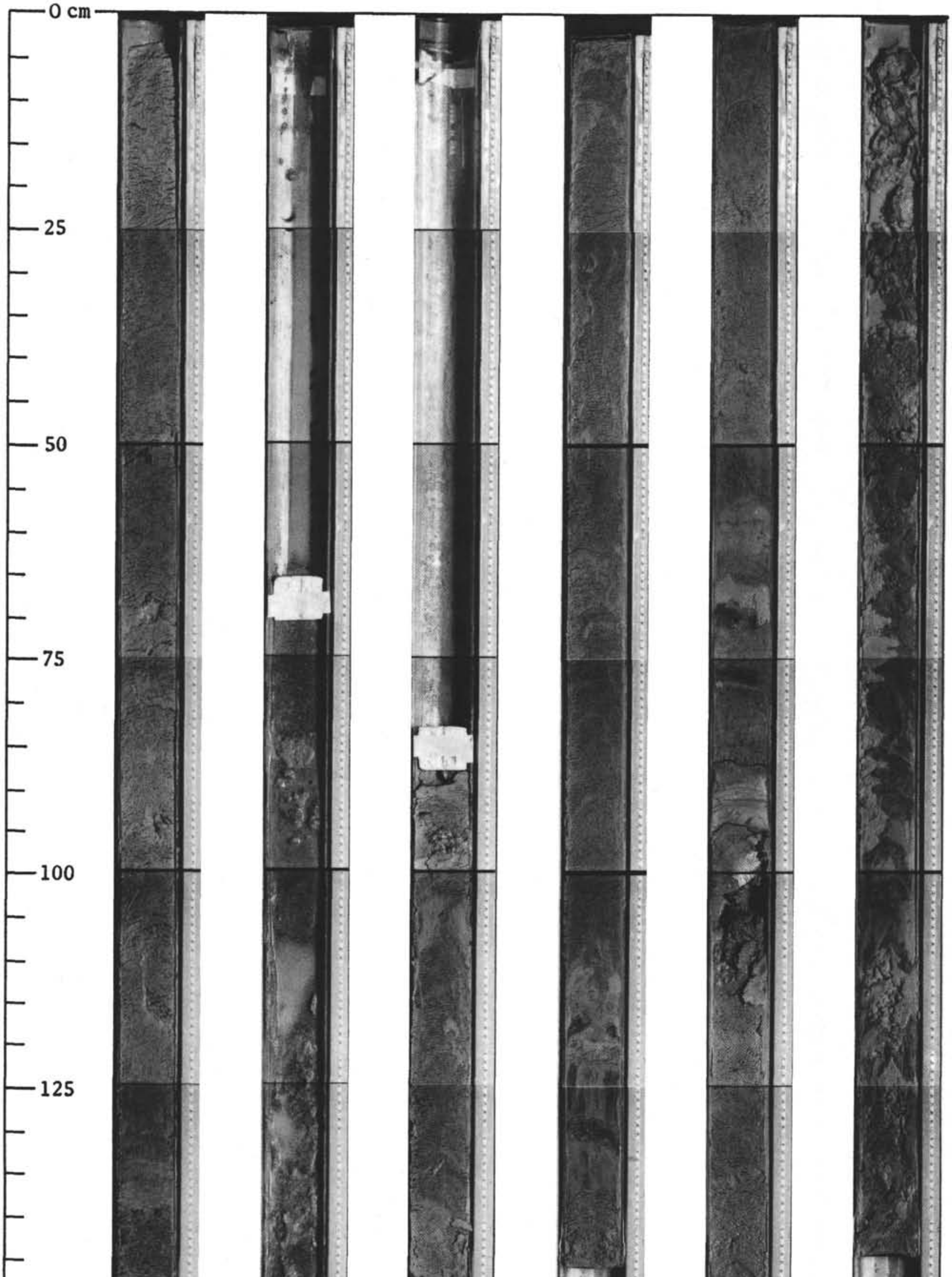
0 cm
25
50
75
100
125
150
297-16-2
297-16-3
297-17-1
297-17-2
297-17-3
297-18-1

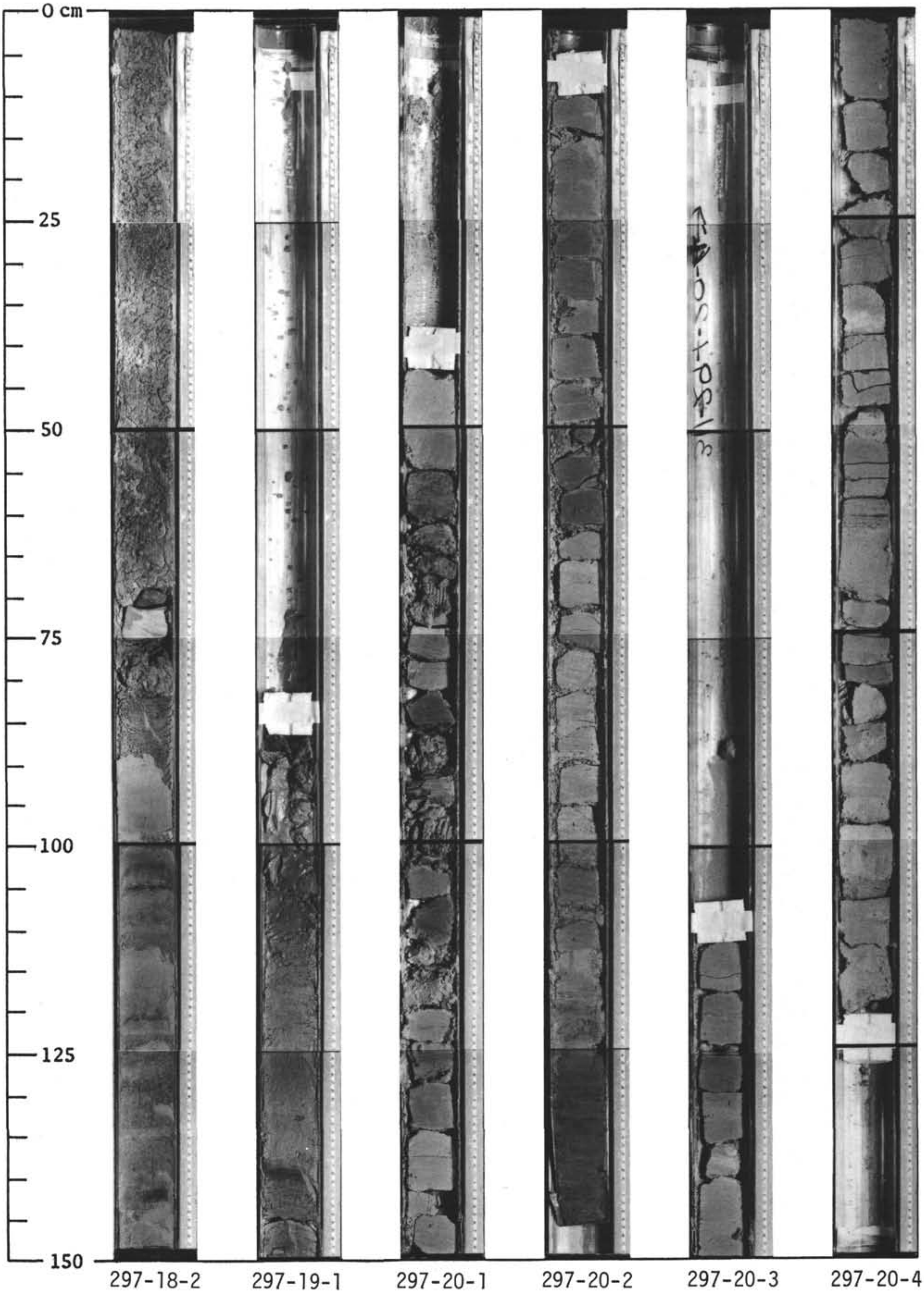
0 cm
25
50
75
100
125
150
297-18-2
297-19-1
297-20-1
297-20-2
297-20-3
297-20-4

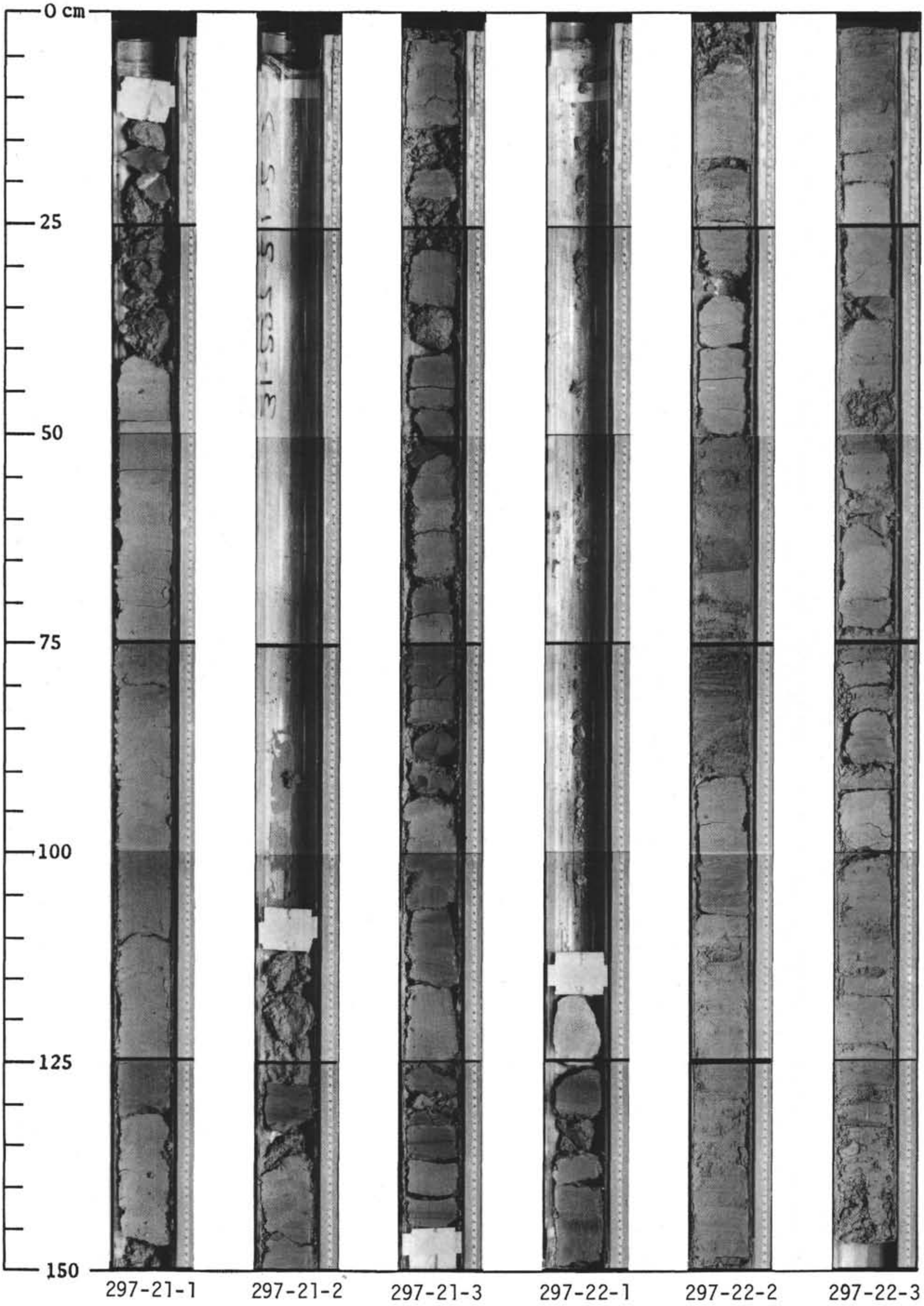
0 cm
25
50
75
100
125
150
297-21-1
297-21-2
297-21-3
297-22-1
297-22-2
297-22-3

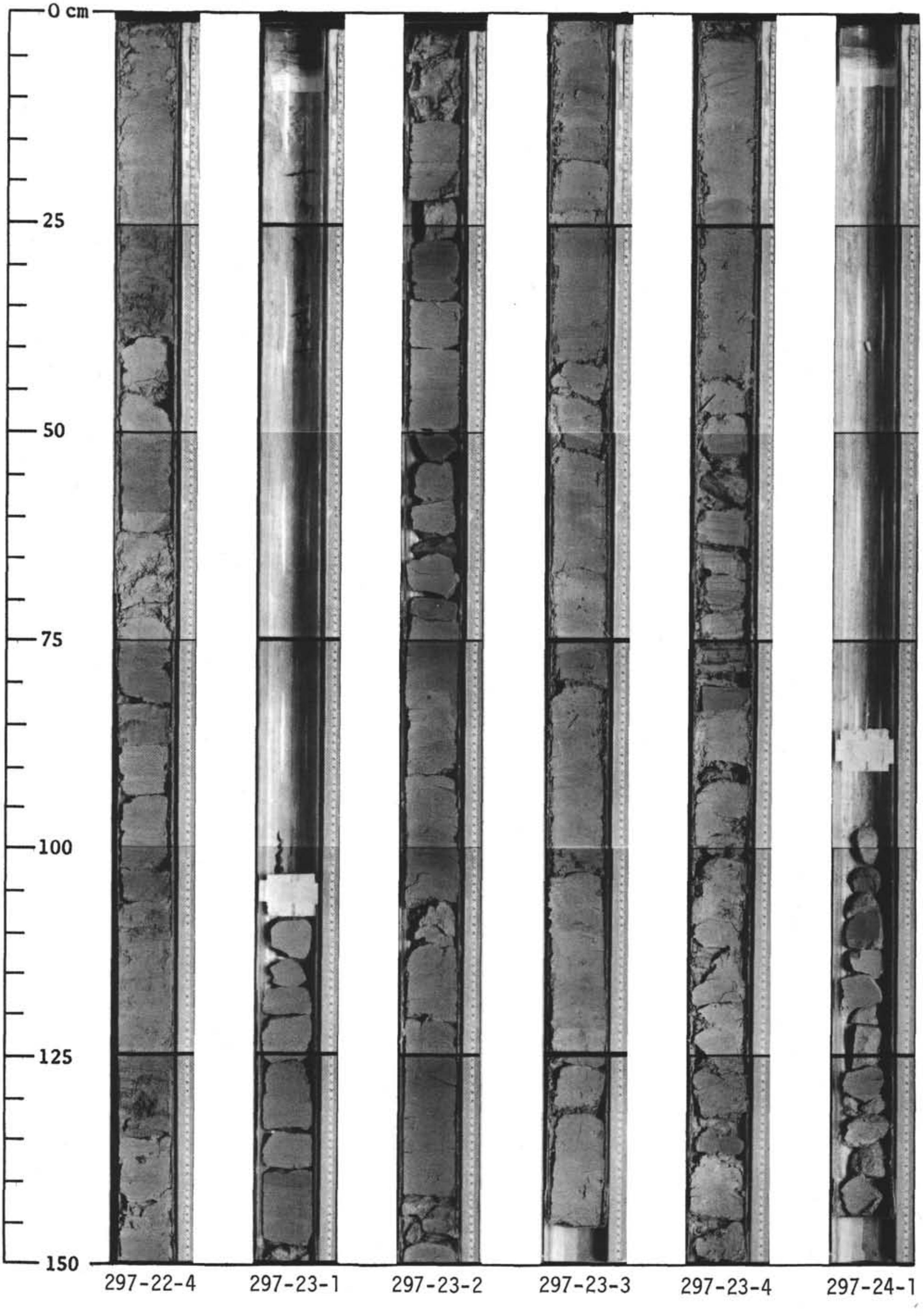
0 cm
25
50
75
100
125
150
297-22-4
297-23-1
297-23-2
297-23-3
297-23-4
297-24-1

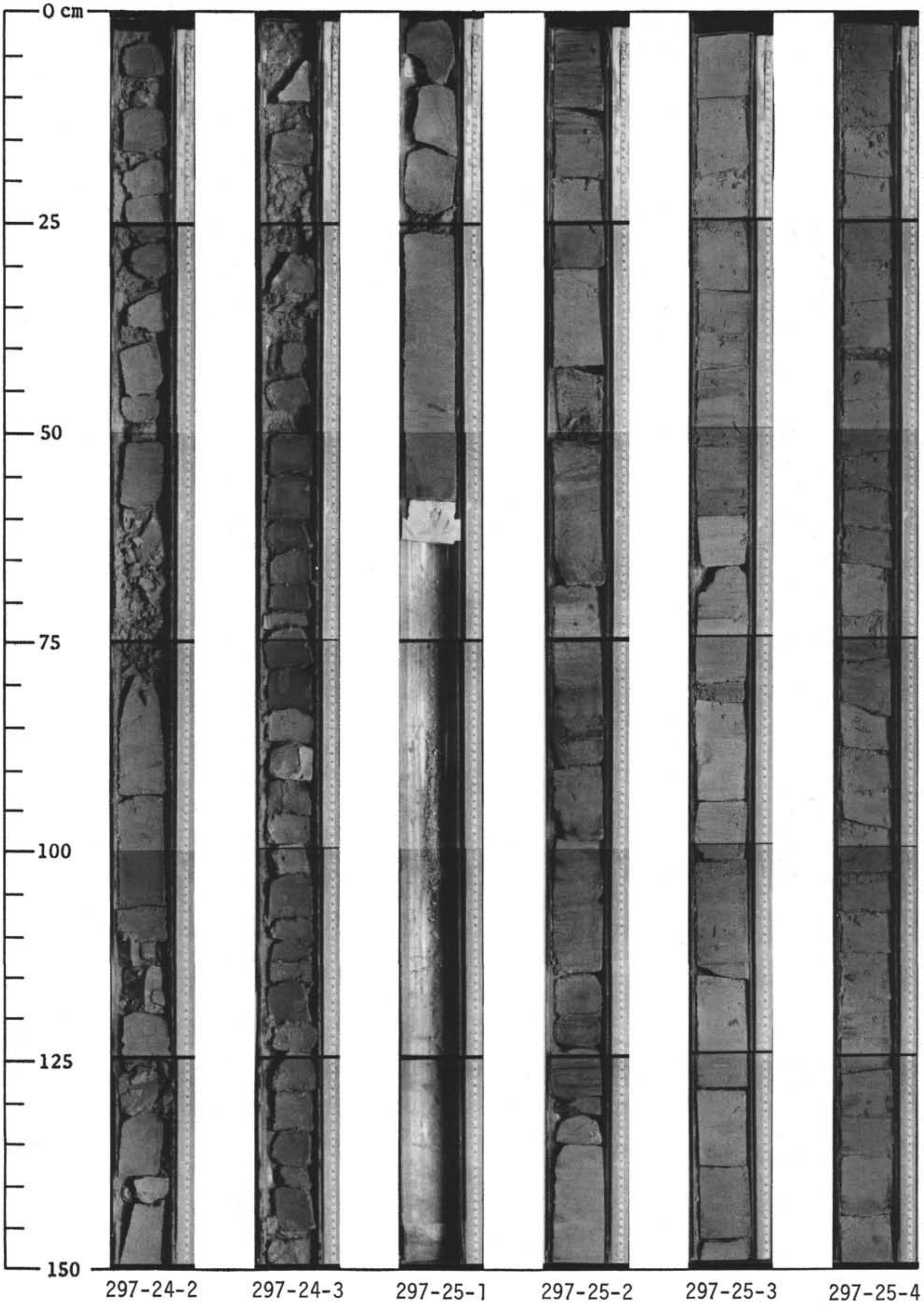
0 cm
25
50
75
100
125
150
297-24-2
297-24-3
297-25-1
297-25-2
297-25-3
297-25-4

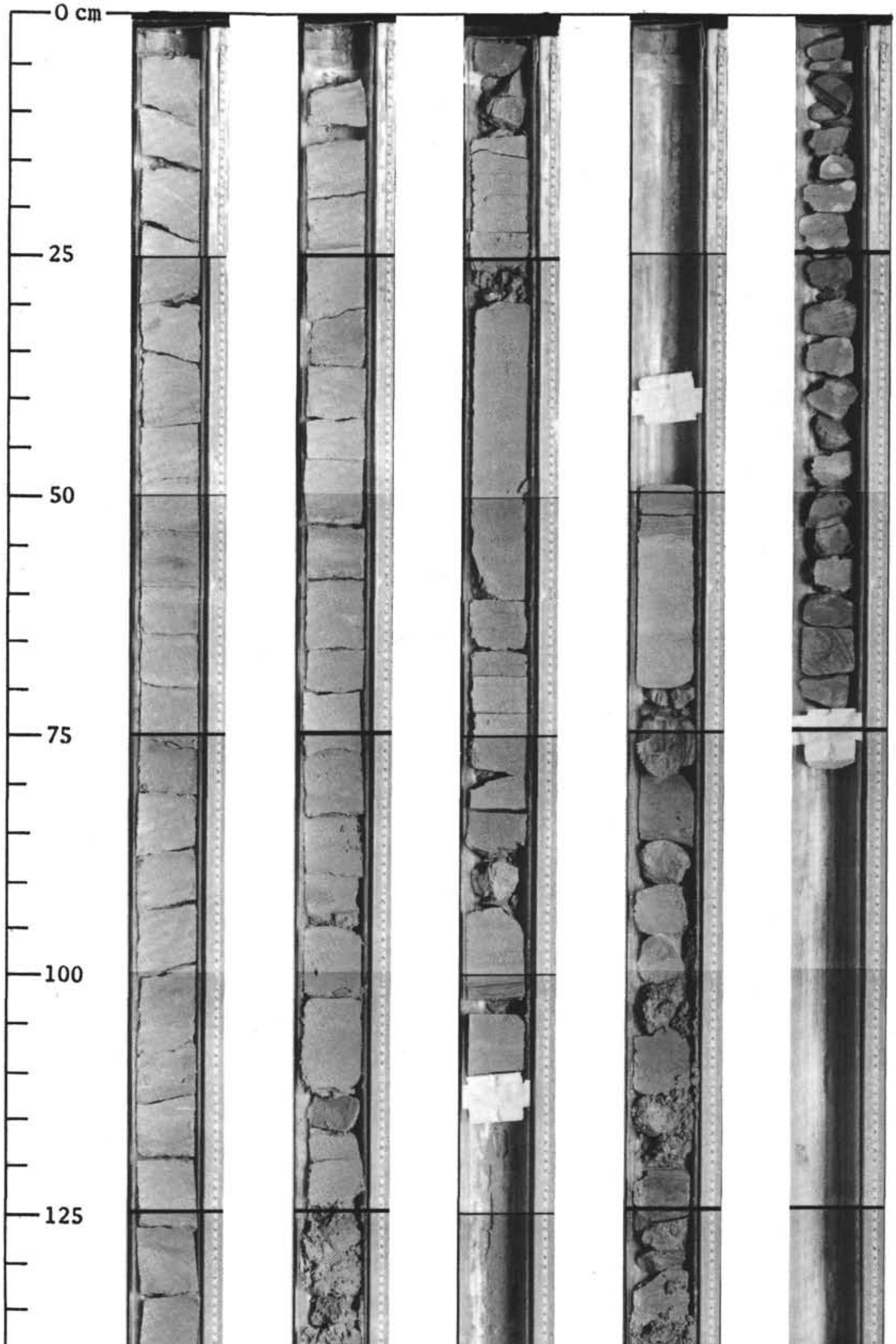
0 cm
25
50
75
100
125
150
297-25-5
297-25-6
297-26-1
297-26-2
297-27-1